Role of β-glucosidase 2 in aberrant glycosphingolipid metabolism: model of glucocerebrosidase deficiency in zebrafish

Lindsey T. Lelieveld[1], Mina Mirzaian[1], Chi-Lin Kuo[1], Marta Artola[1,2], Maria J. Ferraz[1], Remco E.A. Peter[1], Hisako Akiyama[3], Peter Greimel[3], Richard J.B.H.N. van den Berg[2], Herman S. Overkleeft[2], Rolf G. Boot[1], Annemarie H. Meijer[4], Johannes M.F.G. Aerts[1*]

1) Department of Medical Biochemistry, Leiden Institute of Chemistry, Leiden, the Netherlands

2) Bio-organic Synthesis, Leiden Institute of Chemistry, Leiden, the Netherlands

3) Center for Brain Science, RIKEN, Wako, Japan

4) Institute of Biology Leiden, Leiden University, Leiden, the Netherlands

* To whom correspondence should be addressed.

e-mail: j.m.f.g.aerts@LIC.leidenuniv.nl

Running title: Role of Gba2 in glucocerebrosidase deficiency in zebrafish

Abbreviations: AMP-DNM, N-[5-(adamantan-1-ylmethoxy)pentyl]-1-deoxynojirimycin; ABP, activity-based probe; dpf, days post-fertilization; ERT, enzyme replacement therapy; GalCer, galactosylceramide; GalChol, galactosylated cholesterol; GBA1, glucocerebrosidase; GBA2, β-glucosidase 2; GCS, glucosylceramide synthase; GD, Gaucher disease; GlcCer, glucosylceramide; GlcChol, glucosylated cholesterol; GlcSph, glucosylsphingosine; GSL, glycosphingolipid; SRT, substrate reduction therapy.

Abstract

β-glucosidases (GBA1 [glucocerebrosidase], GBA2, and GBA3) are ubiquitous, essential enzymes. Lysosomal GBA1 and cytosol-facing GBA2 degrade glucosylceramide (GlcCer); GBA1 deficiency causes Gaucher disease (GD), a lysosomal storage disorder characterized by lysosomal accumulation of GlcCer, which is partly converted to glucosylsphingosine (GlcSph). GBA1 and GBA2 also may transfer glucose from GlcCer to cholesterol, yielding glucosylated cholesterol (GlcChol). Here, we aimed to clarify the role of zebrafish Gba2 in glycosphingolipid metabolism during Gba1 deficiency in zebrafish (*Danio rerio*), which are able to survive total Gba1 deficiency. We developed Gba1 and Gba2 zebrafish knockouts (*gba1*$^{-/-}$ and *gba2*$^{-/-}$, respectively) using CRISPR/Cas9, modulated glucosidases genetically and pharmacologically, studied GlcCer metabolism in individual larvae, and explored the feasibility of pharmacologic or genetic interventions. Activity-based probes and quantification of relevant glycolipid metabolites confirmed enzyme deficiency. GlcSph increased in *gba1*$^{-/-}$ larvae (0.09 pmol/fish) but did not increase more in *gba1*$^{-/-}$*:gba2*$^{-/-}$ larvae. GlcCer was comparable in *gba1*$^{-/-}$ and wild-type (WT) larvae but increased in *gba2*$^{-/-}$ and *gba1*$^{-/-}$*:gba2*$^{-/-}$ larvae. Independent of Gba1 status, GlcChol was low in all *gba2*$^{-/-}$ larvae (0.05 vs. 0.18. pmol/fish in WT). Pharmacologic inactivation of zebrafish Gba1 comparably increased GlcSph. Inhibition of glucosylceramide synthase in Gba1-deficient larvae reduced GlcCer and GlcSph, and concomitant inhibition of glucosylceramide synthase and Gba2 with iminosugars also reduced excessive GlcChol. Finally, overexpression of human GBA1 and injection of recombinant GBA1 both decreased GlcSph. We determined that zebrafish larvae offer an attractive model to study glucosidase actions in glycosphingolipid metabolism in vivo, and we identified distinguishing characteristics of zebrafish Gba2 deficiency.

Keywords

Glucocerebrosidase, Gaucher disease, sphingolipids, lysosphingolipids, lipid metabolism, zebrafish

Introduction

The lysosomal glucocerebrosidase (GBA1) is a retaining β-glucosidase degrading the glycosphingolipid glucosylceramide (GlcCer) (1). The enzyme receives considerable interest since its deficiency causes Gaucher disease (GD), a recessively inherited lysosomal storage disorder in which GlcCer accumulates in lysosomes, particularly those of tissue macrophages that transform into Gaucher cells (2, 3). GD patients characteristically develop hepatosplenomegaly, leukopenia, especially thrombocytopenia, and abnormalities in coagulation (4). In more severe cases, neuropathology develops, with oculomotor apraxia as a first sign. In its most severe form, complete lack of GBA1 is associated with an acute failure in skin permeability features, causing the so-called collodion baby with severe ichthyosis (2). Individuals that have a genetic defect in GBA1, or carriers of such a mutation, have a markedly increased risk for developing Parkinson's disease and Lewy-body dementia (5, 6). The molecular mechanisms underlying the complex pathophysiology of GD and the risk imposed by GBA1 abnormalities for α-synucleinopathies are presently unknown. The features and functions of GBA1 are presently extensively investigated. Novel research tools in the field are cell-permeable fluorescent activity-based probes (ABPs) that selectively label retaining β-glucosidases in a mechanism-based manner through covalent binding to the catalytic nucleophile. These allow cross-species visualization of active enzyme molecules *in-vitro*, *in-situ* and *in-vivo* (7, 8). Cyclophellitol derivative **1** (**Figure 1A**), carrying the reporter fluorophore at C8 (cyclophellitol number; corresponding to position C6 in glucose), labels selectively GBA1, arguably because the other human retaining β-glucosidases do not accept the presence of a (bulky) fluorophore at this position (7). Cyclophellitol-aziridine **2** with the fluorophore pointing towards the position occupied by the aglycon of a retaining β-exoglucosidase binds all known cellular human β-glucosidases (GBA1, GBA2 and GBA3) (ABP **2**, **Figure 1A** and **B**) (8).

Several corrections for GBA1 deficiency in GD have been developed and novel therapeutic interventions are still being pursued. For almost three decades, non-neuronopathic (type 1) GD can be treated by enzyme replacement therapy (ERT), a treatment based on chronic intravenous administration of GBA1 with mannose-terminal N-glycans ensuring targeting to macrophages, the primary GlcCer storage cells (3, 9). An alternative therapeutic approach is substrate reduction therapy

(SRT) that aims to reduce the biosynthesis of GlcCer through inhibition of glucosylceramide synthase (GCS) (10). The first SRT agent developed for GD is *N*-butyl-deoxynojirimyicin (Miglustat) that was registered almost two decades ago for treatment of mild to moderate type 1 GD (11). More recently, an improved inhibitor for GCS, Eliglustat (**Figure 1C**), has been developed for treatment of type 1 GD patients (12). At present GCS inhibitors, with improved brain-permeability, have been developed as well as chaperones acting as enzyme stabilizers (3, 13, 14). Moreover, augmentation of GBA1 expression by gene therapy approaches is actively studied in animal models (15).

It has been recently recognized that compensatory mechanisms occur during a GBA1 deficiency (3, 16). For example, in GBA1 deficient lysosomes, accumulating GlcCer is partly converted by lysosomal acid ceramidase to its corresponding sphingoid base, glucosylsphingosine (GlcSph) (17). As a result, GlcSph is massively increased in tissues and plasma of GD patients and GBA1-deficient mice (17, 18). Roles for GlcSph in pathophysiology of Gaucher disease with respect to organomegaly, osteoporosis, risks for multiple myeloma, Parkinson's disease and reduced cerebral vascularization have been proposed (18-22).

The cytosol-facing GBA2, which metabolizes cytosolic GlcCer (23-26), has been recently shown to have transglucosidase activity as well, and is able to produce glucosylated cholesterol (GlcChol) from GlcCer and cholesterol (27). The role of GBA2 in GD pathophysiology is unclear. Excessive GBA2 activity during deficiency of GBA1 appears detrimental in some aspects. For example, genetically ablating GBA2 in a Gaucher mouse model as well as in Niemann-Pick type C (NPC) mice has been shown to ameliorate symptoms (18, 28). Moreover, pharmacological inhibition of GBA2 by administration of low nanomolar iminosugar derivatives (AMP-DNM and L-*ido*-AMP-DNM (29, 30), **Figure 1C**) exerts beneficial effects in NPC mice (28).

Zebrafish (*Danio rerio)* are a popular vertebrate research model because of low-cost maintenance and the ability to produce large clutches of embryos. Zebrafish larvae develop ex-utero, are transparent and pharmacological modulation can be conveniently performed (in 96-well plates) up to 5 days post-fertilization (5 dpf) (31, 32). Another attractive feature of the zebrafish is the molecular and genetic similarity to mammalian models. For example, the zebrafish genome encodes GlcCer-metabolizing enzymes and their activity can be measured with the same fluorogenic substrates as

commonly used for the human and rodent analogues (33). We have shown recently that zebrafish Gba1 and Gba2 react like their human counterparts with available ABPs (33, 34) and exhibit similar inhibitor affinities (33, 35). A complete deficiency of GBA1 causes a fatal skin abnormality in newborn mice and man (36, 37), however the introduction of complete Gba1 deficiency in fish is tolerated (38, 39).

The primary goal of our investigation was to study at organismal level the role of Gba2 in glycosphingolipid metabolism during deficiency of Gba1. For this purpose, we used both genetic and pharmacological approaches to modulate Gba1 and Gba2 and subsequently studied the impact on glycosphingolipid levels in individual zebrafish larvae. In Gba1-deficient fish, either genetic or chemically induced, the most remarkable abnormality is the increase in GlcSph, independent of the Gba2 status. The deficiency of Gba2 in zebrafish larvae leads to reduction of GlcChol, independent of the Gba1 status. As a secondary goal we studied the feasibility of pharmacological and genetic interventions. We demonstrate that inhibition of glucosylceramide synthase prohibits excessive formation of GlcSph and that concomitant inhibition of Gba2 also prevents excessive GlcChol. Overexpression of human GBA1 in Gba1-deficient larvae reduces GlcSph elevation. The same is observed upon infusion of recombinant human GBA1. Altogether, we demonstrate that zebrafish embryos offer an attractive organismal model to study glycosphingolipid abnormalities in genetic and pharmacological models of Gba1 and Gba2 deficiencies and moreover allow the screening of GCS and GBA2 inhibitors regarding corrective effects on lipid abnormalities.

Materials and Methods

Zebrafish

Wild-type (WT) zebrafish (ABTL) were a mixed lineage of WT AB and WT TL genetic background. Injections to generate CRISPR/Cas9 mediated knock-out (KO) zebrafish were performed in ABTL embryos and adult zebrafish were outcrossed to ABTL WT zebrafish. *Gba1* mutant zebrafish were maintained as carriers (heterozygous in gba1 genotype), while *gba2* mutant zebrafish were kept and crossed as KO (homozygous in genotype). *Gba1*$^{-/-}$*:gba2*$^{-/-}$ double mutant larvae were continuously generated from adult zebrafish with a *gba1*$^{+/-}$*: gba2*$^{-/-}$ background.

Zebrafish were housed and maintained at Leiden University, the Netherlands, according to standard protocols (zfin.org). Adult zebrafish were housed at a density of 40-50 adults per tank, on a cycle of 14 hour light and 10 hour dark and at 28 °C. The breeding of fish lines was approved by the local animal welfare committee (Instantie voor Dierwelzijn) of Leiden University and followed the international guidelines specified by the EU animal Protection Directive 2010/63/EU. Experiments were performed on embryos and larvae before the free-feeding stage, not falling under animal experimentation law according the EU animal Protection Directive 2010/63/EU. Larvae of 6 and 7 dpf were used according to project licence AVD1060020184725 held by Dr. R.G. Boot. Embryos and larvae were grown in egg water (60 µg/mL Instant Ocean Sera Marin™ aquarium salts (Sera; Heinsberg, Germany)). During inhibitor incubations, fish were kept in E2 medium (15 mM NaCl, 0.5 mM KCl, 1 mM $MgSO_4$, 150 µM KH_2PO_4, 50 µM Na_2HPO_4, 1 mM $CaCl_2$, 0.7 mM $NaHCO_3$, 0.5 mg/L methylene blue) at 28 °C.

Zebrafish cell culture

Zebrafish embryonic fibroblasts (ZF4 cells, (40)) were cultured at 28 °C with 5 % CO_2 in DMEM/F12 (Sigma-Aldrich Chemie GmbH, St Louis, USA) supplemented with 10 % (v/v) Fetal Calf Serum, 1 % (v/v) Glutamax and 0.1 % (v/v) penicillin/streptomycin. Cells were harvested using trypsin (0.25 % (v/v) trypsin in PBS, no EDTA), washed twice with PBS and cell pellets were stored at -80 °C until use.

Chemicals and reagents

ABP **1** (ME569) (33), ABP **2** (JJB367) (8), compound **3** (ME656) (34), AMP-DNM and L-*ido*-AMP-DNM (30), eliglustat (41), $^{13}C_5$-sphinganine, $^{13}C_5$-sphingosine, $^{13}C_5$-GlcSph, $^{13}C_5$-lyso-globotriaosylceramide (LysoGb3), C17-lysosphingomyelin (LysoSM), $^{13}C_6$-GlcChol and C17-dihydroceramide (27, 42) were synthesized as reported. The standards GlcCer (d18:1/16:0), GalCer (d18:1/16:0), β-D-galactosyl cholesterol (GalChol) were obtained from Avanti Polar lipids (Alabaster, USA) and GlcChol from Sigma-Adrich Chemie GmbH. LC-MS grade methanol, 2-propanol, water, formic acid and HPLC grade chloroform were purchased from Biosolve (Valkenswaard, the Netherlands). LC-MS grade ammonium formate and sodium hydroxide from Sigma-Aldrich, butanol and hydrochloric acid from Merck Millipore (Billerica, USA).

General CRISPR target design

Primers and single guide RNA (sgRNA) sequences were designed, with consideration of genomic variation using the known genetic variation of the GRCz10 annotation (ENSDARG00000076058), and purchased from Integrated DNA technologies (IDT, Leuven, Belgium). The CHOPCHOP web-tool (43, 44) was used with 'GN' or 'NG' as 5' requirements. SgRNA sequences are shown in **Supplemental Table S1**.

Generation of short guide RNA

For the generation of sgRNA a cloning-free protocol was adapted (45) using a target specific oligo (Target **1** and **2** for *gba1* and *gba2*, respectively) and a constant reverse oligo (**Supplemental Table S1**). Target specific and constant oligo were annealed using a ramp program: 95 °C for 5 minutes, subsequently cooled to 85 °C with -2 °C/ sec, cooled from 85 °C to 25 °C with -0.1 °C/ sec and hold at 11 °C. The annealed oligos were extended using T4 DNA polymerase (Invitrogen, Carlsbad, USA) for 1 h at 11 °C. The double strand DNA (dsDNA) template was column purified (Nucleospin PCR and gel clean-up kit, Machinery-Nagel, Düren, Germany) and eluted in 20 µL RNase free H_2O. Approximately 200 ng of template was used for the *in vitro* RNA synthesis in a 5 µL reaction using the MEGAshortscript™ T7 Transcription Kit (Ambion®, Thermo Fisher Scientific, Waltham, USA)

according to manufacturer's protocol. After overnight incubation at 37 °C, dsDNA template was removed by incubation with Turbo DNase (Ambion®, Thermo Fisher Scientific, Waltham, USA). SgRNA was purified by ammonium acetate/ethanol precipitation. After washing with 75 % ethanol, the sgRNA was resuspended in RNase free H_2O, the concentration was determined (DeNovix DS-11, Wilmington, USA), the integrity of the sgRNA was verified on a 1 % agarose gel and stored in 2 µL aliquots at -80 °C until use.

Generation of Cas9 mRNA

The pCS2-nCas9n plasmid was generated as previously described (46). The nCas9n plasmid was linearized using NotI (New England Biolabs, Ipswich, USA) and purified (Nucleospin PCR and gel clean-up kit, Machinery-Nagel Düren, Germany). The SP6 promoter of the plasmid was used in combination with the mMessage mMachine® SP6 kit (Ambion®, Thermo Fisher Scientific, Waltham, USA) to synthesize capped Cas9 mRNA. After 3-4 h of incubation at 37 °C, dsDNA template was removed by incubation with Turbo DNase (mMessage mMachine® SP6). Cas9 mRNA was purified using RNAeasy mini kit (Qiagen, Hilden, Germany). Cas9 mRNA was eluted in RNase free H_2O, the concentration was determined (DeNovix DS-11, Wilmington, USA) and Cas9 mRNA was stored in 2 µL aliquots at -80 °C until use.

Cas9/sgRNA injection

Approximately 1 nL total volume of Cas9 mRNA and sgRNA (200 pg and 150 pg for Cas9 mRNA and sgRNA respectively) were co-injected into the yolk of one-or two-cell stage embryos. The integrity of Cas9 mRNA and sgRNA was checked afterwards by loading 1 µL of residual injection mix on 1 % agarose gel. Embryos were checked regularly for unfertilized and dead embryos and subsequently raised to adulthood to generate founder fish (F0).

Genomic DNA extraction and PCR

Genomic DNA (gDNA) of larvae or fin clips was extracted using QuickExtract ™ (EpiCentre ®, Madison, USA) by incubation at 65 °C for 10 min, followed by incubation at 98 °C for 5 min. Samples were vortexed, diluted with water and centrifuged quickly to spin down all non-processed particles which interfere in the PCR reaction. For rapid screening of genotypes, a high-resolution melt (HRM) analysis was used. The fragment was amplified with IQ SYBR green (Bio-Rad laboratories Inc., Hercules, USA) and specific forward and reverse primers (300 µM each, **Supplemental Table S1**) using a Bio-Rad CFX96 Touch™ Real-Time PCR Detection System (Bio-Rad laboratories Inc., Hercules, USA) and the following conditions: denaturation at 95 °C for 3 min, followed by 40 cycles of amplification (95 °C for 30 sec and 61 °C for 30 sec), imaging the plate after every extension at 61 °C, followed by a hold step at 55 °C for 30 sec and a melt program from 55-95 °C with 0.5 °C per step with imaging the plate every step. Melting curve differences were determined using the melting curve RFU values of WT ABTL genomic DNA as reference group. Experimental samples with a shift in melting curve difference with WT were loaded on 2-2.5 % agarose gel to confirm the presence of insertions or deletions (indels).

For sequencing, genomic DNA of positive samples from the HRM analysis were amplified (**Supplemental Table S1**) with Phusion high-fidelity DNA polymerase (Thermo Fisher Scientific, Waltham, USA) according to the manufacturer's protocol using the following conditions: denaturation at 98 °C for 2 min, followed by 35 cycles of amplification (98 °C for 10 sec, 65 °C for 15 sec and 72 °C for 20 sec) and a final extension at 72 °C for 5 min. PCR product was purified (DNA Clean & Concentrator™, Zymo, Irvine, USA) before Sanger Sequencing using the sequence primers shown in **Supplemental Table S1**.

Generation of *gba1*$^{+/-}$, *gba2*$^{-/-}$ and *gba1*$^{+/-}$:*gba2*$^{-/-}$ zebrafish lines

Founder fish were screened by crossing injected zebrafish to WT fish and subsequent screening of the off-spring for germ-line transmitted mutations. Zebrafish with large and out-of-frame mutations were outcrossed to WT and off-spring was raised to adulthood. F1 adult zebrafish were fin-clipped and

screened for the mutation using the HRM analysis. PCR products of positive samples were sequenced and fish with the desired mutation were maintained.

All F1 heterozygous zebrafish were outcrossed to WT fish at least twice (> F3 heterozygous) before incrossing. *Gba1*$^{+/-}$*(*Δ31 mutation) adult fish were crossed with each other and offspring thereof were used for experiments after genotyping. To generate GBA2-deficient fish, adult F3 *gba2*$^{+/-}$*(*Δ16 mutation) fish with the desired mutation were crossed with each other and screened. Offspring of the F4 homozygous adult *gba2*$^{-/-}$ fish were used for experiments. For heterozygous *gba2* samples, *gba2*$^{-/+}$ larvae were obtained by crossing a *gba2*$^{-/-}$ female with a WT male while *gba2*$^{+/-}$ larvae were obtained by crossing a WT female with *gba2*$^{-/-}$ male.

To obtain *gba1*$^{+/-}$*:gba2*$^{-/-}$ zebrafish, *gba1*$^{+/-}$ adult fish were crossed with *gba2*$^{+/-}$ adult fish and raised to adulthood. Adult fish were screened for the desired mutations as described above. Double heterozygous *gba1*$^{+/-}$*:gba2*$^{+/-}$ fish were crossed with heterozygous *gba2*$^{+/-}$ fish, adult fish were screened to obtain fish with the desired genotype (*gba1*$^{+/-}$*:gba2*$^{-/-}$*)* and the offspring of these fish were used for experiments.

Treatment of fish with inhibitors

Adult fish of WT, *gba1*$^{+/-}$, *gba2*$^{-/-}$ or *gba1*$^{+/-}$*:gba2*$^{-/-}$ genotype were crossed and developing off-spring (8 h post-fertilization) were incubated in 100 µL E2 medium immersed with vehicle (0.1-0.2 % (v/v) DMSO) or inhibitor (in 0.1-0.2 % (v/v) DMSO). For embryos of the gba*1*$^{+/-}$ and *gba1*$^{+/-}$*:gba2*$^{-/-}$ crossings, samples were assigned to their genotype as described above. The Gba1 specific inhibitor **3** (**Figure 1A** (34)) was used at a final concentration of 10 µM in all experiments, the iminosugar inhibitors AMP-DNM (47) and L-*ido*-AMP-DNM (29) at final concentrations of 10, 100 nM, 500 nM or 10 µM and Eliglustat at 200 nM or 1 µM final concentration. At 5 dpf, the larvae were washed three times with E2 medium before genotyping and subsequent labelling with ABPs or extraction of lipids as described above.

JOURNAL OF LIPID RESEARCH ASBMB

Generation of Tol2 mediated transgenesis of hGBA1 zebrafish

The coding sequence of human GBA1 (NCBI code: NM_000157) was amplified using Phusion high-fidelity DNA polymerase with primers described in Supplemental Table S1 and subsequently cloned into pDONR using GATEWAY technology (BP reaction, Invitrogen) according to the manufacturer's instruction. The hGBA1 Tol2 destination vector was obtained by recombining the pDONR-hGBA with a p5E-ubi, p3E-polyA and pDEST-Tol2-crystalEye, from the Tol2 kit (48) using a LR reaction. The plasmid containing the Tol2 transposase sequence was linearized using NotI and purified (Nucleospin PCR and gel clean-up kit). Capped and polyadenylated Tol2 mRNA was generated using the mMessage mMachine® SP6 kit as described above for Cas9 mRNA. Approximately 1 nL total volume of Tol2 mRNA and pDEST-ubi:hGBA (100 pg and 20 pg for Tol2 mRNA and plasmid respectively) were co-injected into the yolk of one-or two-cell stage embryos. At 5 dpf, larvae were screened for the expression of Cyan Fluorescent Protein (CFP) in the lens of the eyes and positive larvae were raised to adulthood. Adult zebrafish were crossed with the gba1$^{+/-}$ carriers, generating ubi:hGBA|Gba1$^{+/-}$ zebrafish which were crossed and offspring were used for experiments.

Injection of gba1$^{-/-}$ fish with Cerezyme

Gba1$^{+/-}$ adults were crossed and off-spring (2 dpf) in the bloodstream (i.e. the vein under the yolk sac directed towards the heart) with 16 or 36 µU rGBA1 (Cerezyme®, 1nL in 25 mM Kpi pH5.2; 1,6-3.6x10^{-5} U/mL; Sanofi Genzyme, Cambridge, USA). No increased lethality was observed after injections in either the yolk or in the bloodstream. At 5dpf, the larvae were collected, genotyped and subsequently labelled with ABPs or lipids were extracted as described above.

Homogenate preparation and protein concentration

ZF4 cell homogenates, oocyte, egg or whole zebrafish embryo homogenates were prepared in potassium phosphate (KPi lysis buffer; 25 mM K_2HPO_4-KH_2PO_4 pH 6.5 + 0.1 % (v/v) Triton-X100 + 25 U/ mL Benzonase® Nuclease (Merck, Darmstadt, Germany)) by sonication (20 % amplitude, 3 sec on, 3 sec off for 4 cycles) using a Vibra-Cell™ VCX 130 (Sonics, Newtown, USA) while on ice.

Total protein concentration of homogenates was determined using Pierce™ BCA protein assay kit (Thermo Fisher Scientific, Waltham, USA) and measured using an EMax® plus microplate reader (Molecular Devices, Sunnyvale, USA).

Labelling of β-glucosidases with activity-based probes

ABP **1** (34) was used for specific labelling of Gba1, whereas for concomitant labelling of the three β-glucosidases Gba1, Gba2 and Gba3, ABP **2** was used (49). A WT homogenate was denatured prior to ABP labelling (lane -) to account for aspecific adhesion.

ZF4 cell homogenate (10 µL, 30 µg protein) was preincubated with 5 µL 300 mM McIlvaine buffer (pH 2-8) for 5 min on ice before addition of ABP **1** (5 µL; 400 nM in MQ with 2 % (v/v) DMSO, final concentration of 100 nM and 0.5 % (v/v) DMSO) or ABP **2** (5 µL; 400 nM in MQ, 2 % (v/v) DMSO, final concentration of 100 nM and 0.5 % (v/v) DMSO). Samples were incubated for 30 min at 28 °C before addition of 5x Laemmli sample buffer (5 µL; 25 % (v/v) 1.25 M Tris-HCL pH 6.8, 50 % (v/v) 100 % glycerol, 10 % (w/v) sodium dodecyl sulfate (SDS), 8 % (w/v) dithiothreitol (DTT) and 0.1 % (w/v) bromophenol blue) and boiled for 5 min at 98 °C.

Zebrafish homogenate (10 µL, 1 zebrafish per incubation) was preincubated with 5 µL 300 mM McIlvaine (pH 2-8) for 5 min on ice before addition of ABP **1** or ABP **2** (5 µL ABP **1**; 4 µM in MQ with 2 % (v/v) DMSO, final concentration of 1 µM and 0.5 % (v/v) DMSO or 5 µL ABP **2**; 800 nM in MQ with 2 % (v/v) DMSO, final concentration of 200 nM and 0.5 % (v/v) DMSO). Samples were incubated for 30 min at 28 °C before addition of 5x Laemmli sample buffer (5 µL) and samples were briefly boiled. Homogenates of zebrafish in different developmental stages (10 µL, 1 egg or embryo per lane) were incubated with 10 µL ABP **1** (2 µM in 150 mM McIlvaine pH 4 with 1 % (v/v) DMSO, final concentration of 1 µM with 0.5 % (v/v) DMSO) or ABP **2** (200 nM in 150 mM McIlvaine pH 6 with 1 % (v/v) DMSO, final concentration of 200 nM and 0.5 % (v/v) DMSO) and incubated for 30 min at 28 °C. After incubation, 5x Laemmli sample buffer (5 µL) was added and samples were boiled for 5 min at 98 °C.

For characterization of the *gba1*, *gba2* and *gba1:gba2* double knockout, individual zebrafish 5 dpf larvae with different genotypes were homogenized in 30 µL KPi buffer using a Dounce homogenizer

(10 s; Pellet pestle motor, Kimble® Kontes). Zebrafish homogenate (10 µL, ⅓ of a zebrafish) was incubated with ABP **1** and ABP **2** as described for the different developmental stages. In the case of experiments using Gba1 knockout and inhibitor **3** treated WT at different agents as well as larvae overexpressing human GBA1 or injected with Cerezyme were lysed in 20 µL KPi buffer. Homogenate (½ of a zebrafish) was used to label active Gba1 with ABP **1** as described above, while human GBA1 was labelled using the optimal conditions for human GBA1 (2 µM in 150 mM McIlvaine pH 5.2 with 0,1 % (v/v) Triton-X100 and 0,2 % (w/v) Sodium Taurocholate and 1 % (v/v) DMSO, final concentration of 1 µM with 0.5 % (v/v) DMSO) (7)**.**

Gel electrophoresis and fluorescence scanning

ABP-labelled protein samples were separated by electrophoresis on 8% (w/v) SDS-PAGE gel for 2 h at 90 V, before scanning the fluorescence of the wet-slab gel with a Typhoon FLA 9500 (GE Healthcare, Chicago, USA; Cy5 (635 nm λ_{EX}, 665 nm λ_{EM}), 750 V, pixel size 100 µm).

Western blot and total protein staining

β-Actin as loading control was visualized by western blot using primary rabbit anti-actin antibody (ab8227, Abcam, Cambridge, UK) at 1:2000 and donkey anti-rabbit Horseradish Peroxidase (HRP)-linked secondary antibody (Bio-Rad laboratories Inc., Hercules, USA) at 1:5000. Chemiluminescence was visualized using a ChemiDocMP imager (Bio-Rad laboratories Inc.) in chemiluminescence settings with an exposure of 1 min. Total protein loading was visualized using Coomassie brilliant blue G250 and scanned on the ChemiDocMP imager.

(Glyco)sphingolipid analysis

Neutral (glyco)sphingolipids, (glyco)sphingoid bases and glycosylated cholesterol (HexChol) were extracted from the same individual zebrafish using an acidic Bligh and Dyer procedure (1:1:0.9 chloroform: methanol: 100 mM formate buffer pH 3.1) according to methods described before (27, 42, 50). To an individual zebrafish was added 20 µL of internal standard mixture (0.1 pmol/µL of $^{13}C_5$-sphinganine, $^{13}C_5$-sphingosine, $^{13}C_5$-GlcSph, $^{13}C_5$-lysoGb3 and C17-lysoSM in methanol), 20 µL of

C17-dihydroceramide (20 pmol/ µL in methanol), 20 µL of $^{13}C_6$-GlcChol (0.1 pmol/ µL in methanol) followed by methanol and chloroform (2:1, v/v). After brief mixing, the samples were left at room temperature for 1 h with occasional stirring and 3x 1 min sonication in a bath sonifier (VWR ultrasonic cleaner usc, Radnor, USA). Samples were centrifuged for 10 min at 13,000 rpm to spin down precipitated proteins. The supernatant was transferred to a clean tube, while excess organic solvent was evaporated and genomic DNA was extracted from the remaining material to validate the genotype. Chloroform and 100mM formate buffer pH 3.1 were added to the supernatant, to a final ratio of 1:1:0.9 methanol: chloroform: formate buffer, to induce separation of phases. The upper phase was used for analysis of lyso(glyco)sphingolipids and the lower phase for analysis of neutral (glyco)sphingolipids and HexChol. After centrifugation, the upper phase was transferred to a clean tube and the lower phase (chloroform phase) was extracted an additional time with methanol and formate buffer. Pooled upper phases were concentrated at 45 °C in an Eppendorf concentrator Plus and a butanol/water (1:1, v/v) extraction was performed. The upper phase (butanol phase) was transferred to a clean tube and concentrated. Lipids were dissolved in 100 µL methanol, stirred, sonicated for 30 sec in a bath sonifier and centrifuged. The supernatant was transferred to a vial for subsequent LC-MS/MS analysis.

The remaining lower chloroform phase was transferred to a clean tube and the interphase was washed with chloroform. The pooled lower chloroform phases were split, whereby one part was used to analyse HexChol and the part for analysis of neutral glycosphingolipids was transferred to a pyrex tube and dried at 45 °C under a gentle stream of nitrogen. De-acylation was performed by adding of 500 µL sodium hydroxide (0.1 M NaOH in methanol) using a microwave-assisted saponification method (50). The samples were cooled and neutralized by adding hydrogen chloride (50 µL of 1 M HCl in methanol) and dried, followed by butanol/water extraction and prepared for LC-MS/MS as described above. For determination of HexChol (27), the other half was concentrated, a butanol/ water extraction was performed and samples were prepared for LC-MS/MS analysis as described above.

Glycosphingolipid analysis was performed from three independent crossings and incubations, extractions and measurements using biological replicates as described in the results section.

For hydrophilic interaction liquid chromatography (HILIC) separation, different individual larvae (n= 3-9) were extracted as described above and lipids were resuspended in acetonitrile:methanol (9:1, v/v) prior to transfer to LC-MS vials.

LC-MS/MS

Measurements were performed using a Waters UPLC-Xevo-TQS micro instrument (Waters Corporation, Milford, USA) in positive mode using an electrospray ionization (ESI source). For measurements of (glyco)sphingoid bases, deacylated neutral (glyco)sphingolipids and HexChol, a BEH C18 column (2.1 x 50 mm with 1.7 µm particle size, Waters) was used with eluents and LC-MS/MS programs as described previously for (glyco)sphingoid bases (42) and HexChol (27) respectively. A BEH HILIC column (2.1 x 100 mm with 1.7 µm particle size, Waters) was used at 30 °C for the separation of lipids with glucosyl and galactosyl moiety. In general, eluent A contained 10 mM ammonium formate in acetonitrile/water (97:3, v/v) and 0.01 % (v/v) formic acid and eluent B consisted of 10 mM ammonium formate in acetonitrile/water (75:15, v/v) and 0.01 % (v/v) formic acid. Lyso- and deacylated glycosphingolipids were eluted in 18 min with a flow of 0.4 mL/ min using the following program: 85 % A from 0-2 min, 85-70 % A from 2-2.5 min, 70 % A from 2.5-5.5 min, 70-60 % A from 5.5-6 min, 60 % A from 6-8 min, 60-0 % A from 8-8.5 min, 0-85 % A from 8.5-9.5 min and re-equilibration of the column with 85 % A from 10-18 min. HexChol was eluted in 18 min with a flow of 0.25 ml/ min using the following program: 100 % A from 0-3 min, 100-0 % A from 3-3.5 min, 0 % A from 3.5-4.5 min, 0-100 % A from 4.5-5 min and re-equilibration with 100 % A from 5-18 min. Data was analysed with MassLynx 4.1 Software (Waters).

Statistics

Statistical analysis were performed using GraphPad Prism (v7.00, GraphPadsoftware, CA, USA) and values are presented as mean ± SD. Lipid data were analysed by One-Way Anova using Dunnett's or Tukey's test as described in the results section. Ns=not significant, * $P< 0.05$, ** $P< 0.01$, *** $P< 0.001$ and **** $P< 0.0001$.

Results

Gba1 and Gba2 of zebrafish: detection with fluorescent ABPs.

Zebrafish have one orthologue of human lysosomal GBA1 (38) and zebrafish Gba1 (UniProt accession P04062) shows 58% identity and 73% similarity to the human GBA1 enzyme. The zebrafish Gba1 protein consists of 518 amino acids with a predicted mass of 58 kDa. The zebrafish orthologue (UniProt accession E7F5W0) of human non-lysosomal β-glucosidase shows 66% identity and 79% similarity to human GBA2 and a predicted mass of 96 kDa (35).

We labelled a homogenate of zebrafish embryonic fibroblasts (ZF4 cell line) (40) and a homogenate of pooled WT zebrafish larvae (5 dpf) with ABPs at different pH (**Figure 1D** and **E**). ABP **1**, a Cy5 fluorescent cyclophellitol-epoxide targeting specifically Gba1, labelled a protein with an apparent molecular weight around 60 kDa in the zebrafish homogenates, most favourable at pH 4.0 (**Figure 1D**, top panel). The observed molecular mass coincides with that of the glycosylated zebrafish orthologue of Gba1 and the optimal labelling at acidic pH is consistent with the pH optimum reported for Gba1 (7). Zebrafish material incubated with ABP **2**, the fluorescent cyclophellitol-aziridine that labels all retaining β-glucosidases (8), revealed additionally to Gba1 also a protein with an apparent molecular weight of about 95 kDa (**Figure 1D** and **E**), coinciding with the predicted molecular weight of zebrafish Gba2.

Next, we labelled homogenates of developing zebrafish embryos, from unfertilized oocytes to 7 dpf zebrafish larvae (-f to 7 dpf, **Figure 1F**). Active Gba1 and Gba2 molecules were already detected in both oocytes and fertilized eggs, suggesting the presence of active β-glucosidases in the yolk of the developing embryo deposited by the adult zebrafish female. The intensity of ABP-labelled Gba2 increased over time (in days), while Gba1 intensity reduced in the developing embryo. Of note, although the presence of very abundant yolk proteins, predominantly isoforms of the phospholipo-glycoprotein vitellogenin (51), influenced the apparent molecular weight of the ABP-labelled enzyme, it did not influence target engagement of the ABP.

Gba1$^{-/-}$ larvae accumulate GlcSph

To obtain a *gba1* mutant zebrafish, an appropriate sgRNA sequence was selected in the first exon of *gba1* (Target 1, **Figure 2A** upper and middle panel). Injection of Cas9 mRNA and sgRNA into the one-cell stage of WT embryos generated a founder fish with a germ-line transmitted deletion of 31 bp in the splice-site region of exon 1 (*gba1*Δ31, **Figure 2A,** lower panel). This founder was subsequently used to generate a heterozygous *gba1*$^{+/-}$ zebrafish line without malformations (**Supplemental Figure S2)**. Homozygous *gba1*$^{-/-}$ mutant larvae were obtained following crossing of the adult *gba1*$^{+/-}$ carriers and characterization of offspring by genotyping.

To validate the *gba1*$^{-/-}$ fish (with Δ31 mutation), their Gba1 status was examined by labelling with ABP **1**. Comparison of WT, heterozygous *gba1*$^{+/-}$ and *gba1*$^{-/-}$ KO larvae labelled with ABP **1** revealed a reduction of the ~60 kDa Gba1 in the *gba1*$^{-/-}$ 5 dpf larvae (**Figure 2B**). Some residual labelled protein at 60 kDa was observed in the homozygous *gba1*$^{-/-}$ larvae argued as the deposition of maternal Gba1 enzyme from the heterozygous female (52).

Mass spectrometry as such does not distinguish between lipids with a glucose or galactose moiety. We used HILIC chromatography to separate glucosyl- and galactosyl-containing lipids of additional larvae and observed that accumulated HexSph is solely GlcSph in 5 dpf larvae, while aberrant HexChol is solely GlcChol. In the case of HexCer about 30 % can be attributed to GalCer in 5 dpf WT zebrafish larvae, whereby GalCer levels do not change upon genetic or pharmacological modulation, and the vast majority being GlcCer, showing aberrant levels upon modulation.

To establish whether Gba1 is truly impaired in *gba1*$^{-/-}$ fish, their glycosphingolipid content was determined. In the 5 dpf *gba1*$^{-/-}$ larvae, total hexosylceramide (HexCer), i.e. GlcCer and/or GalCer, and GlcChol was not significantly increased (**Figure 2C**). In the course of the experiments we used HILIC column chromotography to measure sphingolipids with glucose- and galactose moieties in a separate set of zebrafish larvae. This revealed that in the studied 5 dpf larvae more than 70% of HexCer is GlcCer (**Supplemental Figure S5**). This lipid, like total HexCer, did not significantly accumulate in *gba1*$^{-/-}$ zebrafish larvae. Likewise, HILIC separation revealed that solely GlcSph accumulates in the *gba1*$^{-/-}$ larvae **(Figure 2C** and **Supplemental Figure S5**). No significant difference

was detected for other (glyco)sphingolipids such as sphinganine, sphingosine, dihydroceramide, ceramide, GalCer and dihexosylceramide (**Supplemental Figure S6**).

Next, 5 dpf larvae were dissected into head and body regions and glycosphingolipid levels were determined (**Supplemental Figure S7**). GlcSph and GlcCer levels were significantly increased in both regions. GlcChol was also detected in the brain region in comparable levels to the body region.

To conclude, the prominent accumulation of GlcSph in the mutant fish resembles the marked increase of GlcSph in Gba1-deficient patients and mice (53). Thus, we introduced a functional deficiency in lysosomal Gba1 activity in the *gba1*$^{-/-}$ fish promoting active conversion of accumulating GlcCer to GlcSph.

Deficiency in Gba2 results in prominent decrease in GlcChol

Next, we similarly generated a Gba2 deficient fish. An appropriate sgRNA sequence (Target 2, **Figure 3A**, upper and middle panel) was selected in the third exon of the *gba2* gene and subsequent rounds of screening and crossing resulted in a zebrafish with a 16 bp deletion in exon 3 of *gba2*. This deletion created a premature stop codon (**Figure 3A**, lower panel). Adult homozygous *gba2*$^{-/-}$ zebrafish showed no malformations (**Supplemental Figure S2**) or aberrant behaviour. Moreover, adult homozygous *gba2*$^{-/-}$ zebrafish produced regular sized clutches with normally developing larvae until the free-feeding stage of 5 dpf, suggesting that the male *gba2*$^{-/-}$ fish are fertile in contrast to some strains of GBA2 KO mice (24, 54).

To validate GBA2 deficiency in the *gba2*$^{-/-}$ fish (with Δ16 mutation), enzyme status was examined by ABP **2** labelling. Homogenates of zebrafish larvae of different *gba2* genotypes were incubated with GBA1 specific ABP **1** and broad-spectrum ABP **2**. Homozygous *gba2*$^{-/-}$ fish showed complete absence of ABP-labelled enzyme at 90 kDa, while heterozygous offspring from two different crossings exhibited residual ABP-labelled Gba2 enzyme (**Figure 3B**).

The lipid composition of *gba2*$^{-/-}$ larvae (5 dpf) showed an increase in HexCer, predominately GlcCer **(Figure 3C)**. Additionally, these larvae exhibited a very prominent decrease of HexChol (**Figure 3C**). As observed for GlcSph, HILIC separation revealed that GlcChol is the predominant form of HexChol (>95%) in 5 dpf zebrafish larvae (**Supplemental Figure S8)**. The *gba2*$^{-/-}$ fish

showed no increase in GlcSph and no significant differences were found for other (glyco)sphingolipids such as sphinganine, sphingosine, dihydroceramide, ceramide, GalCer and dihexosylceramide (**Figure 3C** and **Supplemental Figure S6**). The GlcChol reduction was not observed in WT and heterozygous *gba2*$^{+/-}$ larvae. The marked reduction in GlcChol in the *gba2*$^{-/-}$ zebrafish larvae is similar to that observed in Gba2-deficient mice (27). This suggests that zebrafish Gba2 also acts as a transglucosylase similar to rodent and human Gba2, generating GlcChol from GlcCer and cholesterol.

Aberrant GlcSph, GlcCer and GlcChol levels in *gba1*$^{-/-}$*:gba2*$^{-/-}$ larvae.

The *gba1*$^{+/-}$:*gba2*$^{-/-}$ adult carrier zebrafish, used to produce *gba1*$^{-/-}$*:gba2*$^{-/-}$ larvae, did not show malformations (**Supplemental Figure S2**) and gave regular sized clutches. To examine the *gba1*$^{-/-}$*:gba2*$^{-/-}$ double KO zebrafish, we employed the same ABP labelling as described above. As in the respective Gba1 and Gba2 single KO, no Gba2 enzyme was visualized on gel, while a residual ABP-labelled enzyme with a molecular mass comparable to Gba1 was present in the double KO 5 dpf larvae (**Figure 4A**).

(Glyco)sphingolipid analysis of *gba1*$^{-/-}$*:gba2*$^{-/-}$ larvae showed increased HexCer levels, predominantly GlcCer, compared to single *gba1*$^{-/-}$ larvae but similar to that of single *gba2*$^{-/-}$ larvae (**Figure 4B**). Moreover, in the double KO larvae, GlcChol was significantly decreased, similar as observed in *gba2*$^{-/-}$ larvae. Compared to WT larvae, a significant accumulation of GlcSph in *gba1*$^{-/-}$*:gba2*$^{-/-}$ larvae was detected. GlcSph levels in double KO fish tended to be somewhat higher than in the *gba1*$^{-/-}$ larvae **(Figure 4B)**, although developing zebrafish showed considerable variation in rapidly accumulating GlcSph.

Next, we analysed the age-dependence of glycosphingolipid changes in developing embryos, from 8 hpf to 5 dpf (**Figure 4C**). The elevation of GlcSph in the *gba1*$^{-/-}$ and *gba1*$^{-/-}$*:gba2*$^{-/-}$ embryos was detectable from 3 dpf onwards. HexCer (predominantly GlcCer) was found to increase also with age, accumulating more rapidly in the gba2$^{-/-}$ and *gba1*$^{-/-}$*:gba2*$^{-/-}$ embryos. GlcChol increased with age in WT and *gba1*$^{-/-}$ embryos, but remained low (around 0,05 pmol/ fish) in the Gba2-deficient fish. The gradual increase with age of GlcChol suggests that it is formed in the developing embryos. In other

JOURNAL OF LIPID RESEARCH ASBMB

words, its origin is unlikely to be entirely the yolk. Other glycosphingolipids (GalCer and dihexosylceramide) also increased with the age of the embryo independent of genotype (**Supplemental Figure S9)**.

Additional accumulation of GlcSph in chemical induced Gba1-deficient larvae

Adamantyl-cyclophellitol **3**, a recently designed highly specific inhibitor of GBA1, was used to investigate the effect of acute pharmacological induction of Gba1 deficiency (34). Incubation of WT larvae with 10 μM of **3** for 5 days led to a significant increase in GlcSph in the developing larvae (**Figure 5A**) and also in their surrounding water (**Supplemental Figure S10**). Incubation of *gba2*$^{-/-}$ larvae increased GlcSph comparable to WT, which indicates that the increase of GlcSph is independent of the Gba2 status (**Figure 5A**). Incubation of *gba1*$^{-/-}$ and *gba1*$^{-/-}$*:gba2*$^{-/-}$ larvae with the Gba1 specific inhibitor led to a significant increase in GlcSph compared to vehicle treated *gba1*$^{-/-}$ or *gba1*$^{-/-}$*:gba2*$^{-/-}$ larvae (**Figure 5A**). GlcChol was only significantly increased in WT treated larvae, while HexCer was increased in all genotypes incubated with **3** (**Figure 5A** and **Supplemental Figure 11**). A potential explanation is the additional inhibition of maternal Gba1 by compound **3** immediately after fertilization, thereby generating a completely Gba1 deficient fish larvae. Indeed, ABP-labelling of vehicle treated *gba1*$^{-/-}$ backgrounds visualized a 60 kDa protein (**Figure 5B**), while ABP-labelled Gba1 was not visible in any of zebrafish pre-treated with inhibitor **3** (**Figure 5B** and **Supplemental Figure S4B**). Of note, ABP-labelled Gba1 was present in *Gba1*$^{-/-}$ embryos of all ages. (**Figure 5C**). Together, the lipid and ABP data suggest the presence of maternal Gba1 enzyme, which can be inhibited by compound **3**.

Lipid corrections by inhibition of glucosylceramide synthase and Gba2

Next, we studied the feasibility of pharmacological intervention and correction of glycosphingolipid abnormalities of Gba1 deficient zebrafish larvae by substrate reduction therapy using treatment with reported GCS inhibitors as well as concomitant GCS and GBA2 inhibitors.

WT zebrafish embryos were simultaneously incubated with the Gba1 specific inhibitor **3** and the potent specific GCS inhibitor Eliglustat to study Gcs inhibition in a Gba1-deficient background

(**Figure 1C**). Incubation with 1 µM Eliglustat for 5 days led to a decrease in HexCer and the derived lipids GlcSph and HexChol (**Figure 6A**). As for characterization of the genetic knockout larvae, the reduction in HexCer levels was prominently due to a decrease in GlcCer levels, based on our HILIC method performed on additional larvae (**Supplemental Figure S12**).

The iminosugars AMP-DNM and L-*ido*-AMP-DNM have been reported as low nanomolar GBA2 inhibitors, though they also inhibit GCS and GBA1 at a higher concentration (**Figure 1C**)(29). Because the reported potencies are *in-vitro* and *in-situ* IC_{50}, we first recapitulated the enzyme specific inhibition of AMP-DNM and L-*ido*-AMP-DNM in whole WT zebrafish larvae. The embryos were incubated with different concentrations of AMP-DNM (10 nM, 100 nM, 500 nM and 10 µM) and L-*ido*-AMP-DNM (10 nM, 100 nM, 500 nM and 10 µM) and GlcSph, HexCer and GlcChol levels were analysed as ratios relative to vehicle treated WT (**Figure 6B**). At the lowest concentration of 10 nM, both iminosugars already caused an increase in HexCer, but no prominent decrease in GlcChol yet. At the higher concentration of 100 nM, both iminosugars caused almost complete *in-vivo* inhibition of Gba2 as reflected by decreasing GlcChol and simultaneously increasing HexCer (**Figure 6B**). At very high concentrations of AMP-DNM and L-*ido*-AMP-DNM (500 nM and 10 µM), levels of HexCer, predominantly GlcCer, decreased, indicating that Gcs was inhibited as well (**Figure 6B** and **Supplemental Figure S13**). A significant increase in GlcSph was observed at high AMP-DNM concentrations (10 µM, **Figure 6B**), but not in case of L-*ido*-AMP-DNM, which is known to hardly inhibit GBA1.

Next, we analysed the potential of the iminosugars to pharmacologically correct the glycosphingolipid abnormalities in Gba1-deficient zebrafish larvae. WT embryos were simultaneously incubated with **3** and different concentrations of AMP-DNM or L-*ido*-AMP-DNM, and glycosphingolipid levels were analysed as ratio relative to control Gba1-deficient zebrafish larvae incubated with **3** alone. Incubation with 100 nM of AMP-DNM and L-*ido*-AMP-DNM resulted in reduction of GlcChol compared to control (**Figure 6C**), indicating Gba2 inhibition. At this concentration, no reduction of GlcSph was found, indicating that pharmacological inhibition of Gba2 in a Gba1-deficient background fails to correct the accumulation of GlcSph at the developmental stage of 5 days post-fertilization. Using high concentrations of AMP-DNM and L-*ido*-AMP-DNM (10µM,

Figure 6C), both Gba2 and Gcs were inhibited as indicated by the reduction of GlcChol and HexCer, mainly GlcCer levels (**Figure 6C** and **Supplemental figure S12**). At these high concentrations significant reduction in GlcSph also became apparent.

Thus, both Eliglustat and the iminosugars at higher dose were able to pharmacologically correct glycosphingolipid abnormalities in Gba1 deficient whole zebrafish larvae.

Rescue of Gba1 deficiency by expression or injection of human GBA1

Finally, we studied correction of abnormal glycosphingolipid metabolism by introducing human GBA1 to Gb1-deficient zebrafish embryos. Two approaches were used: overexpression of human GBA1 using the Tol2 transposase method (48) and injection of recombinant GBA1 enzyme (Cerezyme®) in the bloodstream of 2 dpf *gba1*$^{-/-}$ zebrafish embryos. The presence of active GBA1 was detected by labelling with ABP **1** (**Figure 7A**). Overexpression in the zebrafish resulted in the presence of human GBA1 with heterogeneous molecular weight, indicating differently glycosylated forms. Infusion of rGBA1 into the embryos led to the presence of one distinct band labelled by the ABP**1** (**Figure 7A**). In the latter experiments variation among individual injected embryos was noted. The significant decrease in GlcSph indicates that both overexpression and infusion of human GBA1 functionally correct the absence of zebrafish Gba1 (**Figure 7B**).

In conclusion, glycosphingolipid abnormalities can be corrected by pharmacological and genetic intervention and corrections can be detected in individual zebrafish samples.

Discussion

The primary goal of our investigation was to study GlcCer metabolism during deficiency of the lysosomal Gba1 in a whole organismal model. For this purpose, we selected developing zebrafish larvae until 5 dpf, an attractive model to investigate genetic disorders, related biochemical abnormalities and pharmacological or genetic correction of the disease. We particularly focussed on the potential role of cytosol-facing Gba2 in compensatory GlcCer metabolism during inadequate Gba1 activity. To generate a deficiency of Gba1 and/or Gba2 in zebrafish we used two different approaches: CRISPR/Cas9 mediated knock out of the Gba1 gene (*gba1*$^{-/-}$ fish) as well as chemical inactivation using specific inhibitors. A Cy5 fluorescent ABP, labelling active Gba1 enzyme molecules through covalent binding to the catalytic nucleophile (7), was used to confirm the genetic knockout of Gba1 in *gba1*$^{-/-}$ fish as well as its complete inactivation by selective Gba1 inhibitor **3** (34). Of note, ABP labelling of active Gba1 in *gba1*$^{-/-}$ and *gba1*$^{-/-}$*gba2*$^{-/-}$ fish in the developing zebrafish embryo pointed to the presence of maternal Gba1. Apparently, maternal Gba1 enzyme is deposited by the heterozygous *gba1*$^{+/-}$ mother in the yolk of the embryo, a phenomenon described earlier for other lysosomal enzymes as well (52).

The viability of *gba1*$^{-/-}$ and *gba1*$^{-/-}$:*gba2*$^{-/-}$ fish deserves notice (38). In man and mice, a complete deficiency of Gba1 is not compatible with terrestrial life due to altered skin permeability causing trans-epidermal water loss (37, 55). Recently the abundant presence of active GBA1 in the stratum corneum of human skin has been visualized by labelling with a specific fluorescent ABP and zymography (56). Fortuitously, different properties of fish skin and habitat allow generation of animals with a Gba1 deficiency.

We have earlier developed mass spectrometric methods, using identical ^{13}C-encoded standards, to sensitively quantify the key lipids of interest during GBA1 deficiency; the primary storage lipid GlcCer and the secondary metabolites GlcSph and GlcChol (27, 42). Mass spectrometry as such does not distinguish between lipids with a glucose or galactose moiety. We used HILIC chromatography to separate glucosyl- and galactosyl-containing lipids of additional larvae and observed that accumulated HexSph is solely GlcSph in 5 dpf larvae, while aberrant HexChol is solely

GlcChol. In the case of HexCer about 30 % can be attributed to GalCer in 5 dpf WT zebrafish larvae, whereby GalCer levels do not change upon genetic or pharmacological modulation, and the vast majority being GlcCer, showing aberrant levels upon modulation.

The observed abnormalities in GlcCer and its metabolites GlcSph and GlcChol in 5 dpf Gba1 deficient larvae in the absence or presence of Gba2 warrant discussion. Total HexCer and the HILIC separated GlcCer were found to be not significantly abnormal in the *gba1*$^{-/-}$ larvae. Apparently, accumulating GlcCer in *gba1*$^{-/-}$ larvae can be alternatively metabolized to GlcSph by acid ceramidase or the presence of maternal enzyme in yolk offers somehow degradative capacity. In contrast, deficiency of Gba2 in the 5 dpf larvae does have a major impact on GlcCer levels. The *gba2*$^{-/-}$ larvae showed a clearly elevated HexCer level (two-fold), which is attributed to an increase in GlcCer levels and potentially accumulates at the cytosolic side of membranes. Combined Gba1 and Gba2 deficiency of does not lead to more prominent HexCer accumulation than deficiency of Gba2 alone.

We assessed the marked elevation of GlcSph, which is from accumulating GlcCer in lysosomes by acid ceramidase (17). The abnormality is exploited for diagnostic purposes and monitoring of GD patients regarding disease progression and correction by therapy (19, 53, 57-59). Prominent accumulation of GlcSph develops in zebrafish with the *gba1*$^{-/-}$ background starting around 2-3 dpf, but not in WT or *gba2*$^{-/-}$ zebrafish larvae. Elevation of GlcSph is also rapidly induced by exposing larvae to the Gba1 suicide inhibitor **3**, independent of their *gba1* and *gba2* genotype. Thus, our data suggest that Gba2 status does not markedly influence GlcSph levels during Gba1 deficiency. This suggests that either the Gba2 activity towards GlcSph is insufficient to significantly reduce GlcSph accumulation formed in 5 dpf zebrafish or that GlcSph insufficiently reaches Gba2. Of note, Mistry and coworkers observed in mice with induced Gba1 deficiency in the white blood cell lineage an increased GlcSph that was not changed by combined Gba2 deficiency, similar to our findings with zebrafish embryos (18).

The occurrence of GlcChol abnormalities in zebrafish impaired in Gba1 and/or Gba2 was assessed. The existence of GlcChol has been noted in chicken and mammalian tissues, while the glucosylated sterol was shown to be metabolized by GBA1 as well as GBA2 (27, 60, 61). Evidence has been presented for mice that GBA1 largely degrades GlcChol to glucose and cholesterol. Contrary,

GBA2 forms GlcChol from GlcCer and cholesterol by transglucosylase activity (27). In case of extreme intralysosomal cholesterol accumulation, as in NPC or chemically induced by U18666A, lysosomal GBA1 actively generates GlcChol via transglucosylation (27). GlcChol levels tended to be elevated in *gba1*$^{-/-}$ and chemically induced Gba1-deficient larvae, in line with Gba1 involvement in GlcChol turnover. While a low level of GlcChol was detected in Gba2 deficient embryos at 8 hpf (0,05 pmol/ fish), similar to WT embryos, GlcChol levels did not increase with age in the Gba2 deficient fish, in contrast to WT embryos. This illustrates the contribution of Gba2 to GlcChol biosynthesis in zebrafish, similarly to earlier observations in mice (27). Taken together, this suggests that sterolglucoside metabolism by Gba1 and Gba2 in the zebrafish is similar to that observed in man and mouse (**Supplemental Table S2**) (27, 62). Given the observed abnormalities in GlcChol during abnormal GlcCer metabolism its physiological significance seems intriguing as well as the role of Gba1 and Gba2 in the molecular function of GlcChol.

The iminosugar Miglustat (*N*-butyl-deoxynojirimycin), a registered oral agent to treat mild type 1 GD, markedly inhibits GBA2 activity at the administered dose (3 times 100 mg daily)(47). A very large number of type 1 GD patients have been treated with Miglustat for more than a decade without major side effects except for intestinal complaints due to inhibition of intestinal glycosidases (63). Apparently, in these individuals GBA2 inhibition has no overt detrimental consequences. Moreover, concurrent deficiency of GBA2 in a mouse model with induced deficiency of GBA1 in the white blood cell lineage has been reported to exert positive effects, such as improvements in visceral, hematologic and skeletal symptoms (18). A beneficial effect of GBA2 deficiency has been also been observed for Niemann-Pick type C (NPC) mice, consistent with the use of the GBA2 inhibitor Miglustat in treatment of this disorder (28). In sharp contrast to all these positive findings regarding reduced GBA2 activity during GBA1 deficiency, loss of function of GBA2 is reported to be associated with hereditary spastic paraplegia and cerebellar ataxia in man (64-66). A very recent study reported that some GBA2-KO mice display a strong locomotor defect, while other animals, with the same mutation but in a different background, show only mild alterations of the gait pattern and no signs of cerebellar defects (54). It thus appears that the outcome of GBA2 deficiency may be subtly influenced by yet poorly understood factors. The recent notion that GBA2 has substrates beyond GlcCer, such as

GlcChol, and potentially other glucosylated metabolites, may ultimately lead to an explanation for the presently puzzling heterogeneity in outcome of GBA2 deficiency. In **Supplemental Table S2** an overview is presented of reported glycosphingolipid abnormalities in different Gba1-, Gba2- and Gba1:Gba2 deficient animals (zebrafish, mice and man). Consistently Gba1 deficiency is associated with elevation of GlcSph and Gba2 deficiency with reduced GlcChol levels.

As final part of our investigation, we evaluated the feasibility of reducing GlcCer synthesis by inhibition of glucosylceramide synthase with potent cell-permeable inhibitors. The GCS specific inhibitor Eliglustat, registered for substrate reduction therapy of type 1 GD, led to the expected reduction of HexCer and concomitant decrease of GlcChol in 5 dpf zebrafish. A slight, but significant, decrease in GlcSph was also observed. The iminosugar L-*ido*-AMP-DNM, inhibiting GCS and GBA2 at high doses, also led to reductions of GlcSph and GlcChol in Gba1-deficient larvae. Thus, developing zebrafish embryos offer an organismal model to screen GCS and GBA2 inhibitors and to assess their corrective effect on lipid abnormalities. Also enzyme replacement therapy was feasible in zebrafish larvae and showed GlcSph correction after injection of recombinant GBA1 with mannos-eterminal N-glycans in the bloodstream of 2 dpf zebrafish embryos.

Finally, genetic overexpression of human GBA1 in the zebrafish Gba1-deficient background ameliorated GlcSph accumulation. This indicates that the zebrafish model is able to synthesize human GBA protein, zebrafish Limp2 is able to transport it to the lysosome and the human GBA1 is functionally active in the lysosome shown by the significant reduction of GlcSph, all at the zebrafish optimal temperature of 28.5 °C.

Our present study has focused on the role of Gba2 in glycosphingolipid metabolism during deficiency of Gba1. It will be of great interest to study in the future the possible physiological implications of lipid abnormalities in mutant fish at adult age. It will be of interest to establish whether lipid laden macrophages also play an important role in the pathophysiology in zebrafish with deficient Gba1, as in Gaucher disease. Of interest is also a careful analysis of skin properties of Gba1-deficient zebrafish given the severe abnormalities observed in mice and man completely lacking GBA1 (36, 37). Finally, investigation of the male gonads of Gba1-deficient zebrafish is warranted given the reported abnormalities in this tissue of GBA2-deficient rodents (24, 67). Earlier investigations by

Zancan *et al.* and Keatinge *et al.* reported impaired bone ossification and microglial activation prior to alpha-synuclein-independent neuronal cell death in Gba1-deficient zebrafish, respectively (38, 39). Our mutant zebrafish with combined β-glucosidase deficiencies offer models to obtain further insight in the potential modulating role of Gba2 during Gba1 deficiency. This is of great interest, particularly since current treatments of GBA1-deficient Gaucher patients may impact on GBA2. For example, the registered drug Miglustat is a nanomolar GBA2 inhibitor (47). The recently approved drug Eliglustat, a potent inhibitor of glucosylceramide synthase, is used for substrate reduction therapy of Gaucher disease (68, 69). This agent - by lowering GlcCer - will likely concomitantly reduce the transglucosylase activity of GBA2 (28). At present it is entirely unclear whether reduction of Gba2 activity during Gba1 deficiency is harmful, beneficial or without consequence.

In conclusion, in zebrafish larvae the inactivation of Gba1 leads to a prominent increase in GlcSph, recently proposed to promote α-synuclein aggregation characteristic for Parkinson's disease (21), and a modest increase of GlcChol. Deficiency of Gba2 causes a modest increase in GlcCer levels and a prominent reduction in GlcChol. These findings are reminiscent to findings made in cultured cells as well as mice and humans treated with iminosugars known to inhibit GBA2 (28, 70). Gba2 inactivation during Gba1 deficiency in zebrafish embryos exhibited only little impact on GlcSph levels but reduced GlcChol levels. Abnormalities in GlcSph and GlcChol levels in zebrafish can be corrected with iminosugar derivatives with inhibitory activity towards glucosylceramide synthase and Gba2 concomitantly. Regarding pathophysiology of Gaucher disease, models of GBA1 deficiency in the mouse are intrinsically more informative than models in zebrafish. The general physiology of mice is far closer to that of humans. However, the use of zebrafish offers some practical advantages such as the ease with which multiple genetic traits can be modified and the role of genetic modifiers can be subsequently studied. It is planned by us to introduce in fish with a Gba1-deficient background other traits (e.g. acid ceramidase deficiency that should prevent formation of GlcSph). In conclusion, zebrafish offer an organismal model to assess lipid abnormalities caused by Gba1 deficiency, the impact of Gba2 and the feasibility of pharmacological intervention.

Acknowledgments

We thank The Netherlands Organization for Scientific Research (NWO−CW, ChemThem grant to J.M.F.G.A. and H.S.O.). We thank Dr. J. Bing for synthesizing ABP **2** used in this study and Arwin Groenewoud for sharing the ZF4 cells and plasmids of the Tol2 kit.

References

1. Brady, R. O., J. N. Kanfer, R. M. Bradley, and D. Shapiro. 1966. Demonstration of a deficiency of glucocerebroside-cleaving enzyme in Gaucher's disease. *The Journal of clinical investigation* **45**: 1112-1115.

2. Beutler, E., and G. A. Grabowski. 2001. Glucosylceramide lipidosis-Gaucher disease. *In* The Metabolic and Molecular Bases of Inherited disease. C. R. Scriver, A. L. Beaudet, W. S. Sly, and D. Valle, editors. McGraw-Hill, New York. 3635-3668.

3. Ferraz, M. J., W. W. Kallemeijn, M. Mirzaian, D. Herrera Moro, A. Marques, P. Wisse, R. G. Boot, L. I. Willems, H. S. Overkleeft, and J. M. Aerts. 2014. Gaucher disease and Fabry disease: new markers and insights in pathophysiology for two distinct glycosphingolipidoses. *Biochimica et biophysica acta* **1841**: 811-825.

4. Hollak, C. E., M. Levi, F. Berends, J. M. Aerts, and M. H. van Oers. 1997. Coagulation abnormalities in type 1 Gaucher disease are due to low-grade activation and can be partly restored by enzyme supplementation therapy. *British Journal of Haematology* **96**: 470-476.

5. Sidransky, E., M. A. Nalls, J. O. Aasly, J. Aharon-Peretz, G. Annesi, E. R. Barbosa, A. Bar-Shira, D. Berg, J. Bras, A. Brice, C. M. Chen, L. N. Clark, C. Condroyer, E. V. De Marco, A. Durr, M. J. Eblan, S. Fahn, M. J. Farrer, H. C. Fung, Z. Gan-Or, T. Gasser, R. Gershoni-Baruch, N. Giladi, A. Griffith, T. Gurevich, C. Januario, P. Kropp, A. E. Lang, G. J. Lee-Chen, S. Lesage, K. Marder, I. F. Mata, A. Mirelman, J. Mitsui, I. Mizuta, G. Nicoletti, C. Oliveira, R. Ottman, A. Orr-Urtreger, L. V. Pereira, A. Quattrone, E. Rogaeva, A. Rolfs, H. Rosenbaum, R. Rozenberg, A. Samii, T. Samaddar, C. Schulte, M. Sharma, A. Singleton, M. Spitz, E. K. Tan, N. Tayebi, T. Toda, A. R. Troiano, S. Tsuji, M. Wittstock, T. G. Wolfsberg, Y. R. Wu, C. P. Zabetian, Y. Zhao, and S. G. Ziegler. 2009. Multicenter analysis of glucocerebrosidase mutations in Parkinson's disease. *New England Journal of Medicine* **361**: 1651-1661.

6. Tsuang, D., J. B. Leverenz, O. L. Lopez, R. L. Hamilton, D. A. Bennett, J. A. Schneider, A. S. Buchman, E. B. Larson, P. K. Crane, J. A. Kaye, P. Kramer, R. Woltjer, W. Kukull, P. T. Nelson, G. A. Jicha, J. H. Neltner, D. Galasko, E. Masliah, J. Q. Trojanowski, G. D. Schellenberg, D. Yearout, H. Huston, A. Fritts-Penniman, I. F. Mata, J. Y. Wan, K. L. Edwards, T. J. Montine, and C. P. Zabetian.

2012. GBA mutations increase risk for Lewy body disease with and without Alzheimer disease pathology. *Neurology* **79**: 1944-1950.

7. Witte, M. D., W. W. Kallemeijn, J. Aten, K. Y. Li, A. Strijland, W. E. Donker-Koopman, A. M. van den Nieuwendijk, B. Bleijlevens, G. Kramer, B. I. Florea, B. Hooibrink, C. E. Hollak, R. Ottenhoff, R. G. Boot, G. A. van der Marel, H. S. Overkleeft, and J. M. Aerts. 2010. Ultrasensitive in situ visualization of active glucocerebrosidase molecules. *Nature chemical biology* **6**: 907-913.

8. Kallemeijn, W. W., K. Y. Li, M. D. Witte, A. R. Marques, J. Aten, S. Scheij, J. Jiang, L. I. Willems, T. M. Voorn-Brouwer, C. P. van Roomen, R. Ottenhoff, R. G. Boot, H. van den Elst, M. T. Walvoort, B. I. Florea, J. D. Codee, G. A. van der Marel, J. M. Aerts, and H. S. Overkleeft. 2012. Novel activity-based probes for broad-spectrum profiling of retaining beta-exoglucosidases in situ and in vivo. *Angewandte Chemie* **51**: 12529-12533.

9. Barton, N. W., F. S. Furbish, G. J. Murray, M. Garfield, and R. O. Brady. 1990. Therapeutic response to intravenous infusions of glucocerebrosidase in a patient with Gaucher disease. *P Natl Acad Sci USA* **87**: 1913-1916.

10. Platt, F. M., M. Jeyakumar, U. Andersson, D. A. Priestman, R. A. Dwek, T. D. Butters, T. M. Cox, R. H. Lachmann, C. Hollak, J. M. Aerts, S. Van Weely, M. Hrebicek, C. Moyses, I. Gow, D. Elstein, and A. Zimran. 2001. Inhibition of substrate synthesis as a strategy for glycolipid lysosomal storage disease therapy. *J Inherit Metab Dis* **24**: 275-290.

11. Cox, T., R. Lachmann, C. Hollak, J. Aerts, S. van Weely, M. Hrebicek, F. Platt, T. Butters, R. Dwek, C. Moyses, I. Gow, D. Elstein, and A. Zimran. 2000. Novel oral treatment of Gaucher's disease with N-butyldeoxynojirimycin (OGT 918) to decrease substrate biosynthesis. *Lancet* **355**: 1481-1485.

12. Shayman, J. A. 2010. ELIGLUSTAT TARTRATE: Glucosylceramide Synthase Inhibitor Treatment of Type 1 Gaucher Disease. *Drugs Future* **35**: 613-620.

13. Jung, O., S. Patnaik, J. Marugan, E. Sidransky, and W. Westbroek. 2016. Progress and potential of non-inhibitory small molecule chaperones for the treatment of Gaucher disease and its implications for Parkinson disease. *Expert Rev Proteomics* **13**: 471-479.

14. Shayman, J. A. 2018. Targeting Glucosylceramide Synthesis in the Treatment of Rare and Common Renal Disease. *Semin Nephrol* **38**: 183-192.

15. Dahl, M., A. Doyle, K. Olsson, J. E. Mansson, A. R. A. Marques, M. Mirzaian, J. M. Aerts, M. Ehinger, M. Rothe, U. Modlich, A. Schambach, and S. Karlsson. 2015. Lentiviral gene therapy using cellular promoters cures type 1 Gaucher disease in mice. *Mol Ther* **23**: 835-844.

16. Aerts, J. M., M. J. Ferraz, M. Mirzaian, P. Gaspar, S. V. Oussoren, P. Wisse, C.-L. Kuo, L. T. Lelieveld, K. Kytidou, M. D. Hazeu, D. E. C. Boer, R. Meijer, M. J. C. van der Lienden, D. H. M. Chao, T. L. Gabriel, J. Aten, H. S. Overkleeft, M. van Eijk, R. G. Boot, and A. R. A. Marques. 2017. Lysosomal Storage Diseases. For Better or Worse: Adapting to Defective Lysosomal Glycosphingolipid Breakdown. *In* eLS. John Wiley & Sons, Ltd. 1-13.

17. Ferraz, M. J., A. R. Marques, M. D. Appelman, M. Verhoek, A. Strijland, M. Mirzaian, S. Scheij, C. M. Ouairy, D. Lahav, P. Wisse, H. S. Overkleeft, R. G. Boot, and J. M. Aerts. 2016. Lysosomal glycosphingolipid catabolism by acid ceramidase: formation of glycosphingoid bases during deficiency of glycosidases. *FEBS Lett* **590**: 716-725.

18. Mistry, P. K., J. Liu, L. Sun, W. L. Chuang, T. Yuen, R. Yang, P. Lu, K. Zhang, J. Li, J. Keutzer, A. Stachnik, A. Mennone, J. L. Boyer, D. Jain, R. O. Brady, M. I. New, and M. Zaidi. 2014. Glucocerebrosidase 2 gene deletion rescues type 1 Gaucher disease. *Proc Natl Acad Sci U S A* **111**: 4934-4939.

19. Lukas, J., C. Cozma, F. Yang, G. Kramp, A. Meyer, A. M. Nesslauer, S. Eichler, T. Bottcher, M. Witt, A. U. Brauer, P. Kropp, and A. Rolfs. 2017. Glucosylsphingosine Causes Hematological and Visceral Changes in Mice-Evidence for a Pathophysiological Role in Gaucher Disease. *Int J Mol Sci* **18**.

20. Nair, S., A. R. Branagan, J. Liu, C. S. Boddupalli, P. K. Mistry, and M. V. Dhodapkar. 2016. Clonal Immunoglobulin against Lysolipids in the Origin of Myeloma. *N Engl J Med* **374**: 555-561.

21. Taguchi, Y. V., J. Liu, J. Ruan, J. Pacheco, X. Zhang, J. Abbasi, J. Keutzer, P. K. Mistry, and S. S. Chandra. 2017. Glucosylsphingosine Promotes alpha-Synuclein Pathology in Mutant GBA-Associated Parkinson's Disease. *J Neurosci* **37**: 9617-9631.

22. Smith, N. J., M. Fuller, J. T. Saville, and T. M. Cox. 2018. Reduced cerebral vascularization in experimental neuronopathic Gaucher disease. *J Pathol* **244**: 120-128.

23. van Weely, S., M. Brandsma, A. Strijland, J. M. Tager, and J. M. Aerts. 1993. Demonstration of the existence of a second, non-lysosomal glucocerebrosidase that is not deficient in Gaucher disease. *Biochimica et biophysica acta* **1181**: 55-62.

24. Yildiz, Y., H. Matern, B. Thompson, J. C. Allegood, R. L. Warren, D. M. Ramirez, R. E. Hammer, F. K. Hamra, S. Matern, and D. W. Russell. 2006. Mutation of beta-glucosidase 2 causes glycolipid storage disease and impaired male fertility. *The Journal of clinical investigation* **116**: 2985-2994.

25. Boot, R. G., M. Verhoek, W. Donker-Koopman, A. Strijland, J. van Marle, H. S. Overkleeft, T. Wennekes, and J. M. Aerts. 2007. Identification of the non-lysosomal glucosylceramidase as beta-glucosidase 2. *J Biol Chem* **282**: 1305-1312.

26. Korschen, H. G., Y. Yildiz, D. N. Raju, S. Schonauer, W. Bonigk, V. Jansen, E. Kremmer, U. B. Kaupp, and D. Wachten. 2013. The non-lysosomal beta-glucosidase GBA2 is a non-integral membrane-associated protein at the endoplasmic reticulum (ER) and Golgi. *J Biol Chem* **288**: 3381-3393.

27. Marques, A. R., M. Mirzaian, H. Akiyama, P. Wisse, M. J. Ferraz, P. Gaspar, K. Ghauharali-van der Vlugt, R. Meijer, P. Giraldo, P. Alfonso, P. Irun, M. Dahl, S. Karlsson, E. V. Pavlova, T. M. Cox, S. Scheij, M. Verhoek, R. Ottenhoff, C. P. van Roomen, N. S. Pannu, M. van Eijk, N. Dekker, R. G. Boot, H. S. Overkleeft, E. Blommaart, Y. Hirabayashi, and J. M. Aerts. 2016. Glucosylated cholesterol in mammalian cells and tissues: formation and degradation by multiple cellular beta-glucosidases. *J Lipid Res* **57**: 451-463.

28. Marques, A. R., J. Aten, R. Ottenhoff, C. P. van Roomen, D. Herrera Moro, N. Claessen, M. F. Vinueza Veloz, K. Zhou, Z. Lin, M. Mirzaian, R. G. Boot, C. I. De Zeeuw, H. S. Overkleeft, Y. Yildiz, and J. M. Aerts. 2015. Reducing GBA2 Activity Ameliorates Neuropathology in Niemann-Pick Type C Mice. *PloS one* **10**: e0135889.

29. Wennekes, T., A. J. Meijer, A. K. Groen, R. G. Boot, J. E. Groener, M. van Eijk, R. Ottenhoff, N. Bijl, K. Ghauharali, H. Song, T. J. O'Shea, H. Liu, N. Yew, D. Copeland, R. J. van den Berg, G. A. van der Marel, H. S. Overkleeft, and J. M. Aerts. 2010. Dual-action lipophilic iminosugar improves

glycemic control in obese rodents by reduction of visceral glycosphingolipids and buffering of carbohydrate assimilation. *Journal of medicinal chemistry* **53**: 689-698.

30. Ghisaidoobe, A. T., R. J. van den Berg, S. S. Butt, A. Strijland, W. E. Donker-Koopman, S. Scheij, A. M. van den Nieuwendijk, G. J. Koomen, A. van Loevezijn, M. Leemhuis, T. Wennekes, M. van der Stelt, G. A. van der Marel, C. A. van Boeckel, J. M. Aerts, and H. S. Overkleeft. 2014. Identification and development of biphenyl substituted iminosugars as improved dual glucosylceramide synthase/neutral glucosylceramidase inhibitors. *Journal of medicinal chemistry* **57**: 9096-9104.

31. Ordas, A., R. J. Raterink, F. Cunningham, H. J. Jansen, M. I. Wiweger, S. Jong-Raadsen, S. Bos, R. H. Bates, D. Barros, A. H. Meijer, R. J. Vreeken, L. Ballell-Pages, R. P. Dirks, T. Hankemeier, and H. P. Spaink. 2015. Testing tuberculosis drug efficacy in a zebrafish high-throughput translational medicine screen. *Antimicrobial agents and chemotherapy* **59**: 753-762.

32. Rennekamp, A. J., and R. T. Peterson. 2015. 15 years of zebrafish chemical screening. *Current opinion in chemical biology* **24C**: 58-70.

33. Kuo, C. L., W. W. Kallemeijn, L. T. Lelieveld, M. Mirzaian, I. Zoutendijk, A. Vardi, A. H. Futerman, A. H. Meijer, H. P. Spaink, H. S. Overkleeft, J. Aerts, and M. Artola. 2019. In vivo inactivation of glycosidases by conduritol B epoxide and cyclophellitol as revealed by activity-based protein profiling. *FEBS J* **286**: 584-600.

34. Artola, M., C. L. Kuo, L. T. Lelieveld, R. J. Rowland, G. A. van der Marel, J. D. C. Codee, R. G. Boot, G. J. Davies, J. Aerts, and H. S. Overkleeft. 2019. Functionalized Cyclophellitols Are Selective Glucocerebrosidase Inhibitors and Induce a Bona Fide Neuropathic Gaucher Model in Zebrafish. *Journal of the American Chemical Society* **141**: 4214-4218.

35. Sultana, S., N. Y. Truong, D. B. Vieira, J. G. Wigger, A. M. Forrester, C. J. Veinotte, J. N. Berman, and A. C. van der Spoel. 2016. Characterization of the Zebrafish Homolog of beta-Glucosidase 2: A Target of the Drug Miglustat. *Zebrafish* **13**: 177-187.

36. Sidransky, E., D. M. Sherer, and E. I. Ginns. 1992. Gaucher disease in the neonate: a distinct Gaucher phenotype is analogous to a mouse model created by targeted disruption of the glucocerebrosidase gene. *Pediatr Res* **32**: 494-498.

37. Holleran, W. M., E. I. Ginns, G. K. Menon, J. U. Grundmann, M. Fartasch, C. E. McKinney, P. M. Elias, and E. Sidransky. 1994. Consequences of beta-glucocerebrosidase deficiency in epidermis. Ultrastructure and permeability barrier alterations in Gaucher disease. *The Journal of clinical investigation* **93**: 1756-1764.

38. Keatinge, M., H. Bui, A. Menke, Y. C. Chen, A. M. Sokol, Q. Bai, F. Ellett, M. Da Costa, D. Burke, M. Gegg, L. Trollope, T. Payne, A. McTighe, H. Mortiboys, S. de Jager, H. Nuthall, M. S. Kuo, A. Fleming, A. H. Schapira, S. A. Renshaw, J. R. Highley, A. Chacinska, P. Panula, E. A. Burton, M. J. O'Neill, and O. Bandmann. 2015. Glucocerebrosidase 1 deficient Danio rerio mirror key pathological aspects of human Gaucher disease and provide evidence of early microglial activation preceding alpha-synuclein-independent neuronal cell death. *Human molecular genetics* **24**: 6640-6652.

39. Zancan, I., S. Bellesso, R. Costa, M. Salvalaio, M. Stroppiano, C. Hammond, F. Argenton, M. Filocamo, and E. Moro. 2015. Glucocerebrosidase deficiency in zebrafish affects primary bone ossification through increased oxidative stress and reduced Wnt/beta-catenin signaling. *Human molecular genetics* **24**: 1280-1294.

40. Driever, W., and Z. Rangini. 1993. Characterization of a cell line derived from zebrafish (Brachydanio rerio) embryos. *In Vitro Cell Dev Biol Anim* **29A**: 749-754.

41. McEachern, K. A., J. Fung, S. Komarnitsky, C. S. Siegel, W. L. Chuang, E. Hutto, J. A. Shayman, G. A. Grabowski, J. M. Aerts, S. H. Cheng, D. P. Copeland, and J. Marshall. 2007. A specific and potent inhibitor of glucosylceramide synthase for substrate inhibition therapy of Gaucher disease. *Mol Genet Metab* **91**: 259-267.

42. Mirzaian, M., P. Wisse, M. J. Ferraz, A. R. A. Marques, P. Gaspar, S. V. Oussoren, K. Kytidou, J. D. C. Codee, G. van der Marel, H. S. Overkleeft, and J. M. Aerts. 2017. Simultaneous quantitation of sphingoid bases by UPLC-ESI-MS/MS with identical (13)C-encoded internal standards. *Clin Chim Acta* **466**: 178-184.

43. Montague, T. G., J. M. Cruz, J. A. Gagnon, G. M. Church, and E. Valen. 2014. CHOPCHOP: a CRISPR/Cas9 and TALEN web tool for genome editing. *Nucleic acids research* **42**: W401-407.

44. Labun, K., T. G. Montague, J. A. Gagnon, S. B. Thyme, and E. Valen. 2016. CHOPCHOP v2: a web tool for the next generation of CRISPR genome engineering. *Nucleic acids research* **44**: W272-276.

45. Gagnon, J. A., E. Valen, S. B. Thyme, P. Huang, L. Akhmetova, A. Pauli, T. G. Montague, S. Zimmerman, C. Richter, and A. F. Schier. 2014. Efficient mutagenesis by Cas9 protein-mediated oligonucleotide insertion and large-scale assessment of single-guide RNAs. *PloS one* **9**: e98186.

46. Jao, L. E., S. R. Wente, and W. Chen. 2013. Efficient multiplex biallelic zebrafish genome editing using a CRISPR nuclease system. *Proc Natl Acad Sci U S A* **110**: 13904-13909.

47. Overkleeft, H. S., G. H. Renkema, J. Neele, P. Vianello, I. O. Hung, A. Strijland, A. M. van der Burg, G. J. Koomen, U. K. Pandit, and J. M. Aerts. 1998. Generation of specific deoxynojirimycin-type inhibitors of the non-lysosomal glucosylceramidase. *J Biol Chem* **273**: 26522-26527.

48. Kwan, K. M., E. Fujimoto, C. Grabher, B. D. Mangum, M. E. Hardy, D. S. Campbell, J. M. Parant, H. J. Yost, J. P. Kanki, and C. B. Chien. 2007. The Tol2kit: a multisite gateway-based construction kit for Tol2 transposon transgenesis constructs. *Developmental dynamics : an official publication of the American Association of Anatomists* **236**: 3088-3099.

49. Schroder, S. P., J. W. van de Sande, W. W. Kallemeijn, C. L. Kuo, M. Artola, E. J. van Rooden, J. Jiang, T. J. M. Beenakker, B. I. Florea, W. A. Offen, G. J. Davies, A. J. Minnaard, J. Aerts, J. D. C. Codee, G. A. van der Marel, and H. S. Overkleeft. 2017. Towards broad spectrum activity-based glycosidase probes: synthesis and evaluation of deoxygenated cyclophellitol aziridines. *Chemical communications* **53**: 12528-12531.

50. Groener, J. E., B. J. Poorthuis, S. Kuiper, M. T. Helmond, C. E. Hollak, and J. M. Aerts. 2007. HPLC for simultaneous quantification of total ceramide, glucosylceramide, and ceramide trihexoside concentrations in plasma. *Clin Chem* **53**: 742-747.

51. Link, V., A. Shevchenko, and C. P. Heisenberg. 2006. Proteomics of early zebrafish embryos. *BMC Dev Biol* **6**: 1.

52. Fan, X., M. Klein, H. R. Flanagan-Steet, and R. Steet. 2010. Selective yolk deposition and mannose phosphorylation of lysosomal glycosidases in zebrafish. *J Biol Chem* **285**: 32946-32953.

53. Dekker, N., L. van Dussen, C. E. Hollak, H. Overkleeft, S. Scheij, K. Ghauharali, M. J. van Breemen, M. J. Ferraz, J. E. Groener, M. Maas, F. A. Wijburg, D. Speijer, A. Tylki-Szymanska, P. K. Mistry, R. G. Boot, and J. M. Aerts. 2011. Elevated plasma glucosylsphingosine in Gaucher disease: relation to phenotype, storage cell markers, and therapeutic response. *Blood* **118**: e118-127.

54. Woeste, M. A., S. Stern, D. N. Raju, E. Grahn, D. Dittmann, K. Gutbrod, P. Dormann, J. N. Hansen, S. Schonauer, C. E. Marx, H. Hamzeh, H. G. Korschen, J. Aerts, W. Bonigk, H. Endepols, R. Sandhoff, M. Geyer, T. K. Berger, F. Bradke, and D. Wachten. 2019. Species-specific differences in nonlysosomal glucosylceramidase GBA2 function underlie locomotor dysfunction arising from loss-of-function mutations. *J Biol Chem* **294**: 3853-3871.

55. Farfel-Becker, T., E. B. Vitner, and A. H. Futerman. 2011. Animal models for Gaucher disease research. *Dis Model Mech* **4**: 746-752.

56. van Smeden, J., I. M. Dijkhoff, R. W. J. Helder, H. Al-Khakany, D. E. C. Boer, A. Schreuder, W. W. Kallemeijn, S. Absalah, H. S. Overkleeft, J. Aerts, and J. A. Bouwstra. 2017. In situ visualization of glucocerebrosidase in human skin tissue: zymography versus activity-based probe labeling. *J Lipid Res* **58**: 2299-2309.

57. Rolfs, A., A. K. Giese, U. Grittner, D. Mascher, D. Elstein, A. Zimran, T. Bottcher, J. Lukas, R. Hubner, U. Golnitz, A. Rohle, A. Dudesek, W. Meyer, M. Wittstock, and H. Mascher. 2013. Glucosylsphingosine is a highly sensitive and specific biomarker for primary diagnostic and follow-up monitoring in Gaucher disease in a non-Jewish, Caucasian cohort of Gaucher disease patients. *PloS one* **8**: e79732.

58. Mirzaian, M., P. Wisse, M. J. Ferraz, H. Gold, W. E. Donker-Koopman, M. Verhoek, H. S. Overkleeft, R. G. Boot, G. Kramer, N. Dekker, and J. M. Aerts. 2015. Mass spectrometric quantification of glucosylsphingosine in plasma and urine of type 1 Gaucher patients using an isotope standard. *Blood Cells Mol Dis* **54**: 307-314.

59. Arkadir, D., T. Dinur, S. Revel-Vilk, M. Becker Cohen, C. Cozma, M. Hovakimyan, S. Eichler, A. Rolfs, and A. Zimran. 2018. Glucosylsphingosine is a reliable response biomarker in Gaucher disease. *Am J Hematol* **93**: E140-E142.

60. Wertz, P. W., P. M. Stover, W. Abraham, and D. T. Downing. 1986. Lipids of chicken epidermis. *J Lipid Res* **27**: 427-435.

61. Akiyama, H., K. Nakajima, Y. Itoh, T. Sayano, Y. Ohashi, Y. Yamaguchi, P. Greimel, and Y. Hirabayashi. 2016. Aglycon diversity of brain sterylglucosides: structure determination of cholesteryl- and sitosterylglucoside. *J Lipid Res* **57**: 2061-2072.

62. Akiyama, H., and Y. Hirabayashi. 2017. A novel function for glucocerebrosidase as a regulator of sterylglucoside metabolism. *Biochim Biophys Acta Gen Subj* **1861**: 2507-2514.

63. Giraldo, P., M. Andrade-Campos, P. Alfonso, P. Irun, K. Atutxa, A. Acedo, A. Barez, M. Blanes, V. Diaz-Morant, M. A. Fernandez-Galan, R. Franco, C. Gil-Cortes, V. Giner, A. Ibanez, P. Latre, I. Loyola, E. Luno, R. Hernandez-Martin, B. Medrano-Engay, J. Puerta, I. Roig, J. de la Serna, O. Salamero, L. Villalon, and M. Pocovi. 2018. Twelve years of experience with miglustat in the treatment of type 1 Gaucher disease: The Spanish ZAGAL project. *Blood Cells Mol Dis* **68**: 173-179.

64. Hammer, M. B., G. Eleuch-Fayache, L. V. Schottlaender, H. Nehdi, J. R. Gibbs, S. K. Arepalli, S. B. Chong, D. G. Hernandez, A. Sailer, G. Liu, P. K. Mistry, H. Cai, G. Shrader, C. Sassi, Y. Bouhlal, H. Houlden, F. Hentati, R. Amouri, and A. B. Singleton. 2013. Mutations in GBA2 cause autosomal-recessive cerebellar ataxia with spasticity. *Am J Hum Genet* **92**: 245-251.

65. Martin, E., R. Schule, K. Smets, A. Rastetter, A. Boukhris, J. L. Loureiro, M. A. Gonzalez, E. Mundwiller, T. Deconinck, M. Wessner, L. Jornea, A. C. Oteyza, A. Durr, J. J. Martin, L. Schols, C. Mhiri, F. Lamari, S. Zuchner, P. De Jonghe, E. Kabashi, A. Brice, and G. Stevanin. 2013. Loss of function of glucocerebrosidase GBA2 is responsible for motor neuron defects in hereditary spastic paraplegia. *Am J Hum Genet* **92**: 238-244.

66. Woeste, M. A., and D. Wachten. 2017. The Enigmatic Role of GBA2 in Controlling Locomotor Function. *Front Mol Neurosci* **10**: 386.

67. Raju, D., S. Schonauer, H. Hamzeh, K. C. Flynn, F. Bradke, K. Vom Dorp, P. Dormann, Y. Yildiz, C. Trotschel, A. Poetsch, B. Breiden, K. Sandhoff, H. G. Korschen, and D. Wachten. 2015. Accumulation of glucosylceramide in the absence of the beta-glucosidase GBA2 alters cytoskeletal dynamics. *Plos Genet* **11**: e1005063.

68. Cox, T. M., G. Drelichman, R. Cravo, M. Balwani, T. A. Burrow, A. M. Martins, E. Lukina, B. Rosenbloom, O. Goker-Alpan, N. Watman, A. El-Beshlawy, P. S. Kishnani, M. L. Pedroso, S. J. M. Gaemers, R. Tayag, and M. J. Peterschmitt. 2017. Eliglustat maintains long-term clinical stability in patients with Gaucher disease type 1 stabilized on enzyme therapy. *Blood* **129**: 2375-2383.

69. Mistry, P. K., E. Lukina, H. Ben Turkia, S. P. Shankar, H. Baris, M. Ghosn, A. Mehta, S. Packman, G. Pastores, M. Petakov, S. Assouline, M. Balwani, S. Danda, E. Hadjiev, A. Ortega, S. J. M. Gaemers, R. Tayag, and M. J. Peterschmitt. 2017. Outcomes after 18 months of eliglustat therapy in treatment-naive adults with Gaucher disease type 1: The phase 3 ENGAGE trial. *Am J Hematol* **92**: 1170-1176.

70. Ashe, K. M., D. Bangari, L. Li, M. A. Cabrera-Salazar, S. D. Bercury, J. B. Nietupski, C. G. Cooper, J. M. Aerts, E. R. Lee, D. P. Copeland, S. H. Cheng, R. K. Scheule, and J. Marshall. 2011. Iminosugar-based inhibitors of glucosylceramide synthase increase brain glycosphingolipids and survival in a mouse model of Sandhoff disease. *PloS one* **6**: e21758.

Figures

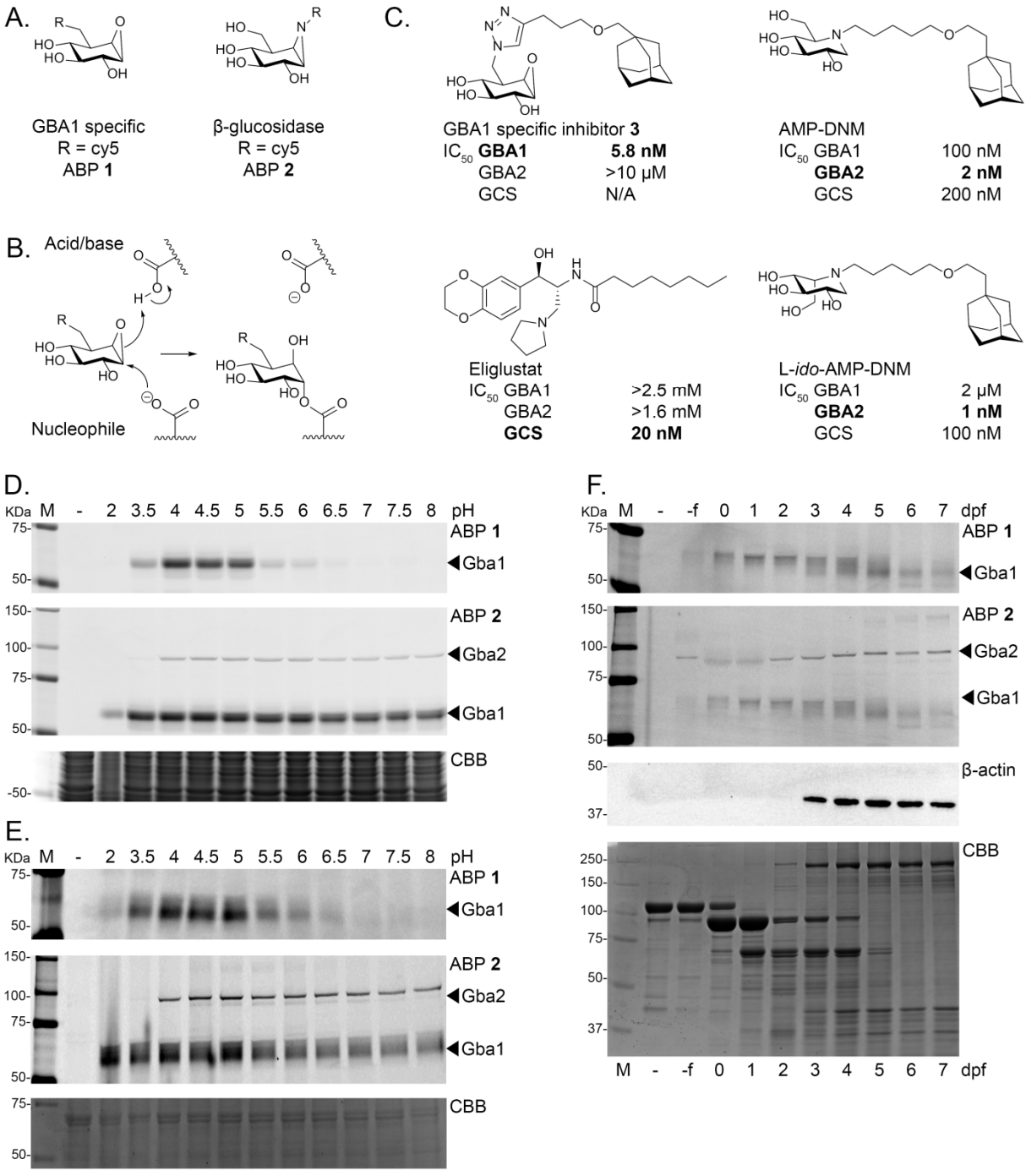

Figure 1 | Visualization of active Gba1 and Gba2 enzyme in zebrafish

(A) Chemical structures of activity-based probes (ABPs) used in this study: cyclophellitol-epoxide-based ABP **1** (GBA1 specific) and cyclophellitol-aziridine-based ABP **2** (labelling all retaining β-glucosidases). Both ABPs are equipped with a Cy5 fluorophore as reporter. (B) Catalytic reaction mechanism of cyclophellitol-based irreversible inhibitors. (C) Chemical structures of the GBA1 specific irreversible inhibitor **3** (ME656), iminosugars AMP-DNM and L-*ido*-AMP-DNM and

Eliglustat. IC_{50} values are given for GBA1 and GBA2 and GCS (29, 34). (D) Effect of pH on labelling of ZF4 cell homogenate with ABP **1** (100 nM) and ABP **2** (100 nM). (E) Effect of pH on labelling of pooled zebrafish homogenate (5 dpf) with ABP **1** (1 µM) and ABP **2** (200 nM). A protein equivalent of one zebrafish was used per condition. (F) ABP **1** and ABP **2** labelling of homogenate of oocytes (-f) and developing zebrafish embryos (t = 0-7 dpf). An equivalent of one zebrafish egg or embryo was used per lane. In lane –, sample is denatured prior to ABP addition, Coomassie Brilliant Blue (CBB) staining and β-actin were used as loading controls.

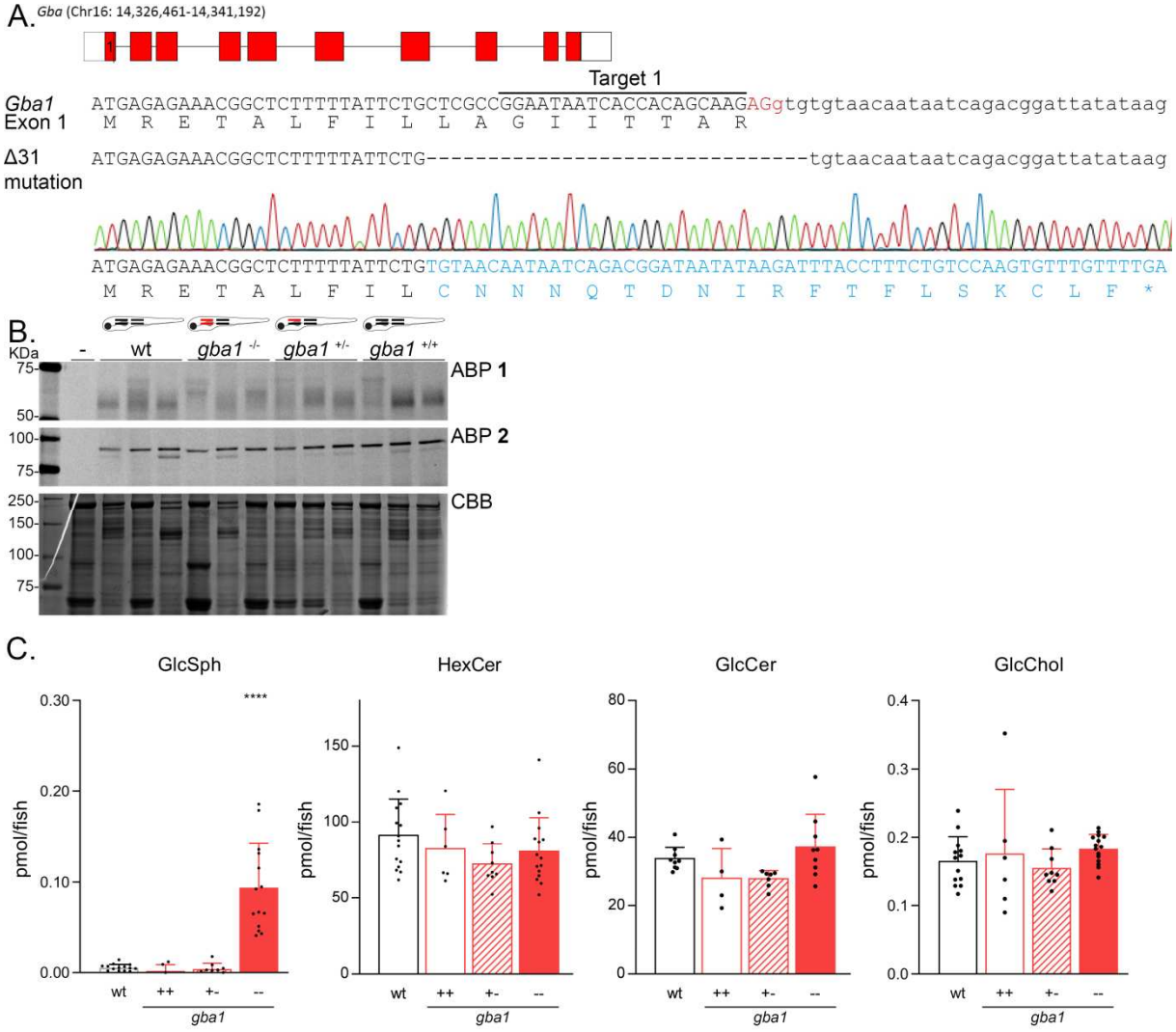

Figure 2 | CRISPR/Cas9 mediated disruption of Gba1 in zebrafish

(A) Top panel: Schematic representation of the *gba1* gene on chromosome 16. Middle panel: DNA sequence of the exon1-intron1 boundary of *gba1* with the exon in upper case and intron in lower case,

JOURNAL OF LIPID RESEARCH
ASBMB

the sgRNA target sequence underlined, the PAM site in red and the protein sequence shown below. Lower panel: The 31 base pair deletion (Δ31), obtained from the sequence trace of an homozygous *gba1*Δ31 larvae, is located in the splice-region with the altered predicted translated protein sequence given in blue and leads to a premature stopcodon (*). (B) ABP labelling of homogenate of individual zebrafish larvae at 5 dpf (WT, $gba1^{-/-}$, $gba1^{+/-}$ or $gba1^{+/+}$ from incross, n= 3) with ABP **1** (top panel) or ABP **2** (middle panel). In lane –, sample is denatured prior to ABP addition, CBB staining was used as loading control. (C) GlcSph, HexCer, GlcCer and GlcChol levels were determined of individual zebrafish larvae in pmol/ fish; WT (n = 15), $gba1^{+/+}$ (n = 6), $gba1^{+/-}$ (n = 9) and $gba1^{-/-}$ (n = 15) for GlcSph, HexCer and GlcChol and WT (n = 9), $gba1^{+/+}$ (n = 4), $gba1^{+/-}$ (n = 7) and $gba1^{-/-}$ (n = 9) for GlcCer. Data is depicted as mean ± SD and analysed using One-Way Anova (Dunnett's test) with WT as control group with **** $P < 0.0001$.

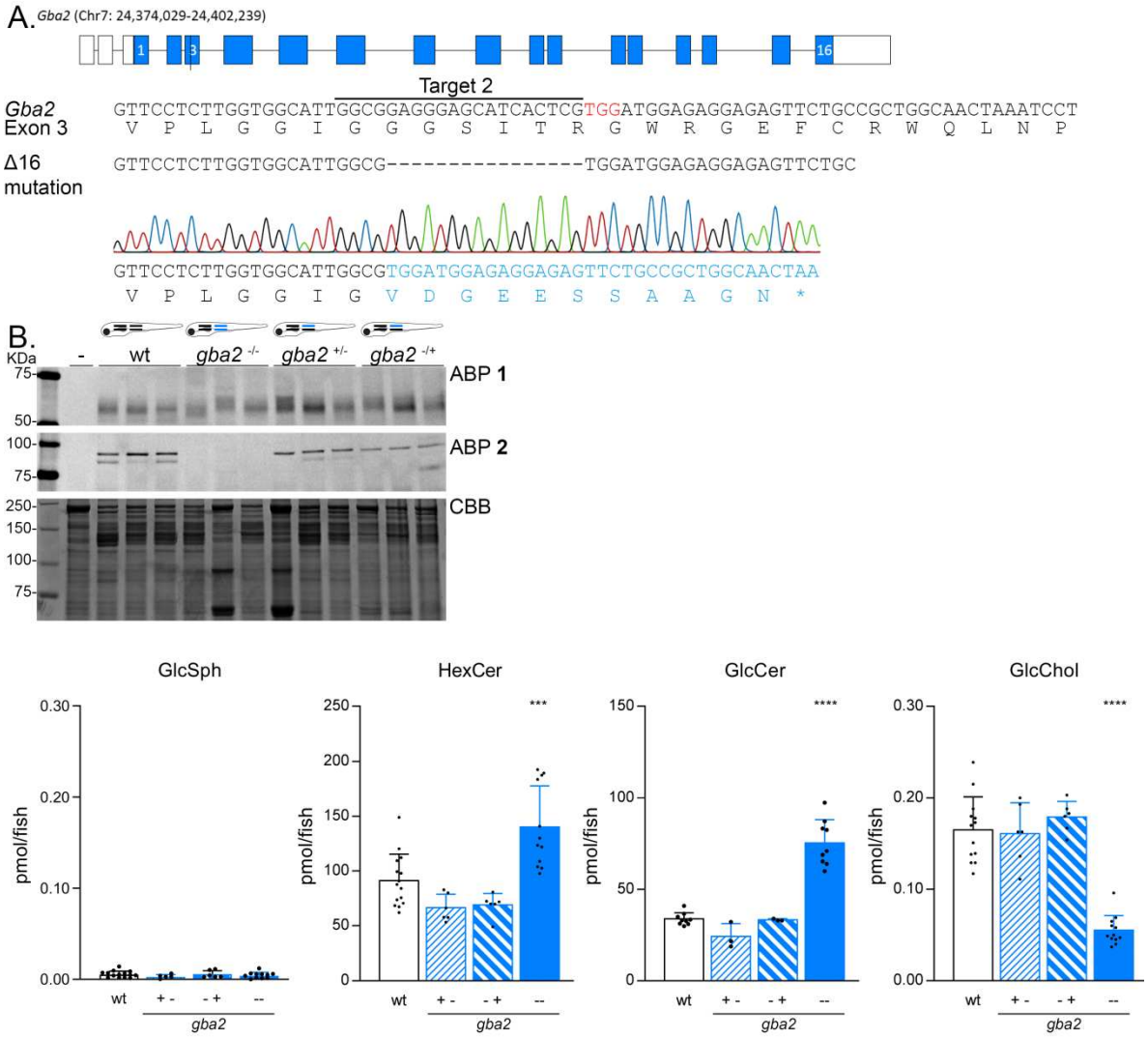

Figure 3 | CRISPR/Cas9 mediated disruption of Gba2 in zebrafish.

(A) Top panel: Schematic representation of *gba2* gene on chromosome 7. Middle panels: DNA sequence of exon 3 of *gba2* with the sgRNA target sequence underlined, the PAM site in red and the protein sequence shown below. Lower panel: The 16 base pair deletion (Δ16), as obtained from the sequence trace, introduces a premature stopcodon (*) in the altered predicted translated protein sequence, given in blue. (B) ABP labelling of homogenate of individual zebrafish larvae at 5 dpf (WT, *gba2*$^{-/-}$ and both heterozygous *gba2*$^{+/-}$ options, n= 3) with ABP **1** (top panel) or ABP **2** (middle panel). In lane –, sample is denatured prior to ABP addition, CBB staining was used as loading control. C) GlcSph, HexCer, GlcCer and GlcChol levels were determined of individual zebrafish larvae in pmol/ fish; WT (n = 15), *gba2*$^{+/-}$ (n = 6), *gba2*$^{-+-}$ (n = 6) and *gba2*$^{-/-}$ (n = 12) for GlcSph, HexCer and GlcChol and WT (n = 9), *gba2*$^{+/-}$ (n = 3), *gba2*$^{-+-}$ (n = 3) and *gba2*$^{-/-}$ (n = 9) for GlcCer. Data is

depicted as mean ± SD and analysed using One-Way Anova (Dunnett's test) with wt as control group with *** $P < 0.001$ and **** $P < 0.0001$.

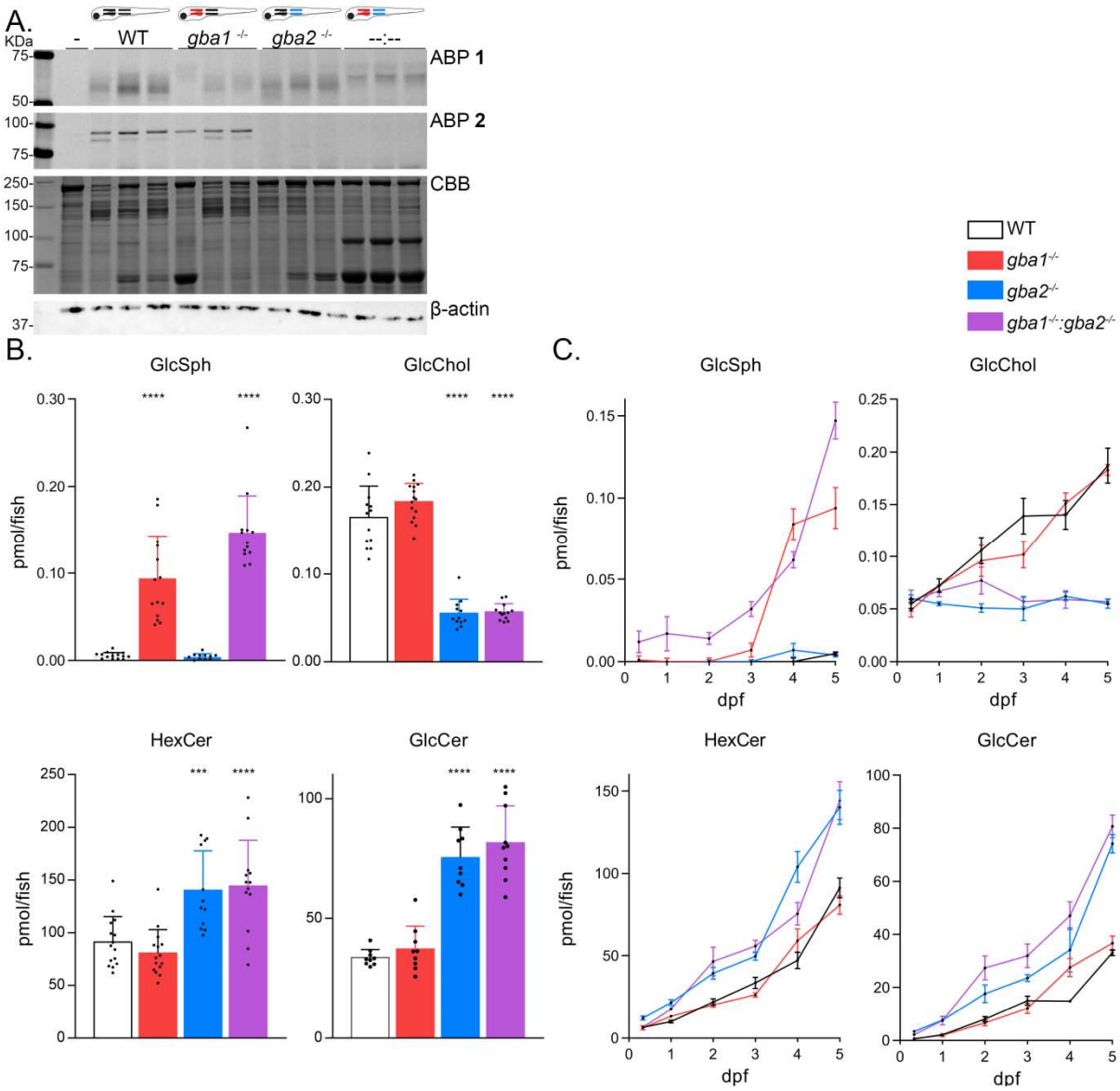

Figure 4 | Biochemical evaluation of *gba1*, *gba2* and double *gba1*:*gba2* KO zebrafish larvae

(A) ABP labelling of homogenate of individual zebrafish larvae at 5 dpf (WT, *gba1*$^{-/-}$, *gba2*$^{-/-}$ and *gba1*$^{-/-}$:*gba2*$^{-/-}$, n = 3) with ABP **1** (top panel) or ABP **2** (middle panel). In lane –, sample is denatured prior to ABP addition, CBB staining and β-actin were used as loading control (lower panels). (B) GlcSph, HexCer, GlcCer and GlcChol levels were determined of individual 5dpf zebrafish larvae in pmol/fish; WT (n = 15), *gba1*$^{-/-}$ (n = 15), *gba2*$^{-/-}$ (n = 12) and *gba1*$^{-/-}$:*gba2*$^{-/-}$ (n = 13) for GlcSph, HexCer and GlcChol and WT (n = 9), *gba1*$^{-/-}$ (n = 9), *gba2*$^{-/-}$ (n = 9) and *gba1*$^{-/-}$:*gba2*$^{-/-}$ (n = 10) for GlcCer. Data is depicted as mean ± SD and analysed by One-Way Anova (Dunnett's test) with WT as

control group. * $P < 0.05$, ** $P < 0.01$, *** $P < 0.001$ and **** $P < 0.0001$. (C) Developing zebrafish embryos were harvested at different ages and GlcSph, HexCer, GlcCer and GlcChol levels were determined in pmol/ fish. 8 hours post fertilization (n = 4-5), 1 dpf (n = 3-5), 2 dpf (n = 3-5), 3 dpf (n = 3-5), 4 dpf (n = 3-6). Data on relevant lipid levels of 5 dpf larvae are obtained from (C). Data is depicted as mean ± SEM

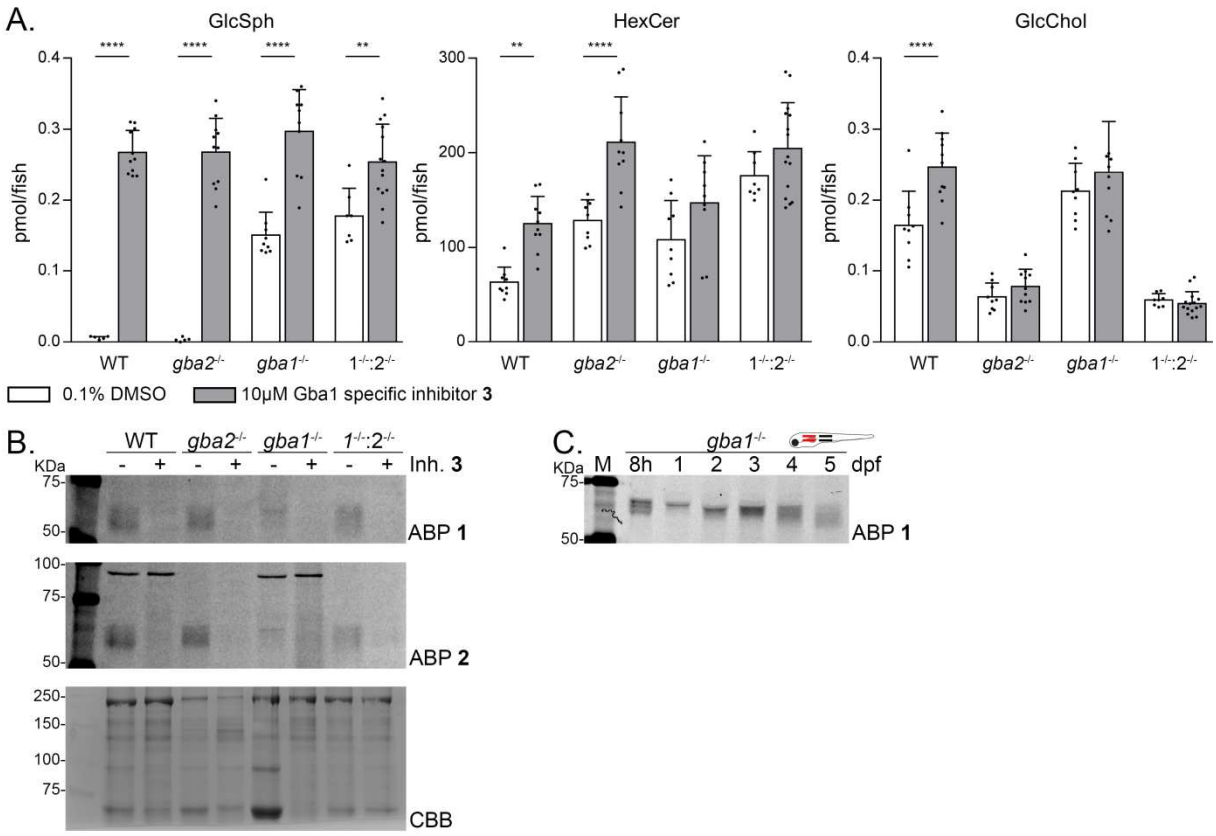

Figure 5 | Chemical inactivation of Gba1 shows full gba1 deficiency with increased GlcSph levels

WT, *gba2*$^{-/-}$, *gba1*$^{-/-}$ and *gba1*$^{-/-}$*:gba2*$^{-/-}$ embryos were treated with vehicle (0.1 % (v/v) DMSO) or inhibitor **3** (10 µM) for 5 days and (A) relevant lipid levels were determined of individual larvae in pmol/ fish (n = 7-15) or (B) active β-glucosidase enzyme was visualized with ABP **1** (top panel) or ABP **2** (middle panel); CBB staining was used as loading control (lower panel). (C) *Gba1*$^{-/-}$ embryos were harvested at different ages and active Gba1 was visualized with ABP **1**. Data of GlcSph, HexCer and GlcChol is depicted as mean ± SD and analysed using One-Way Anova (Tukey's test). Ns= not significant, * $P < 0.05$, ** $P < 0.001$, *** $P < 0.001$ and **** $P < 0.0001$.

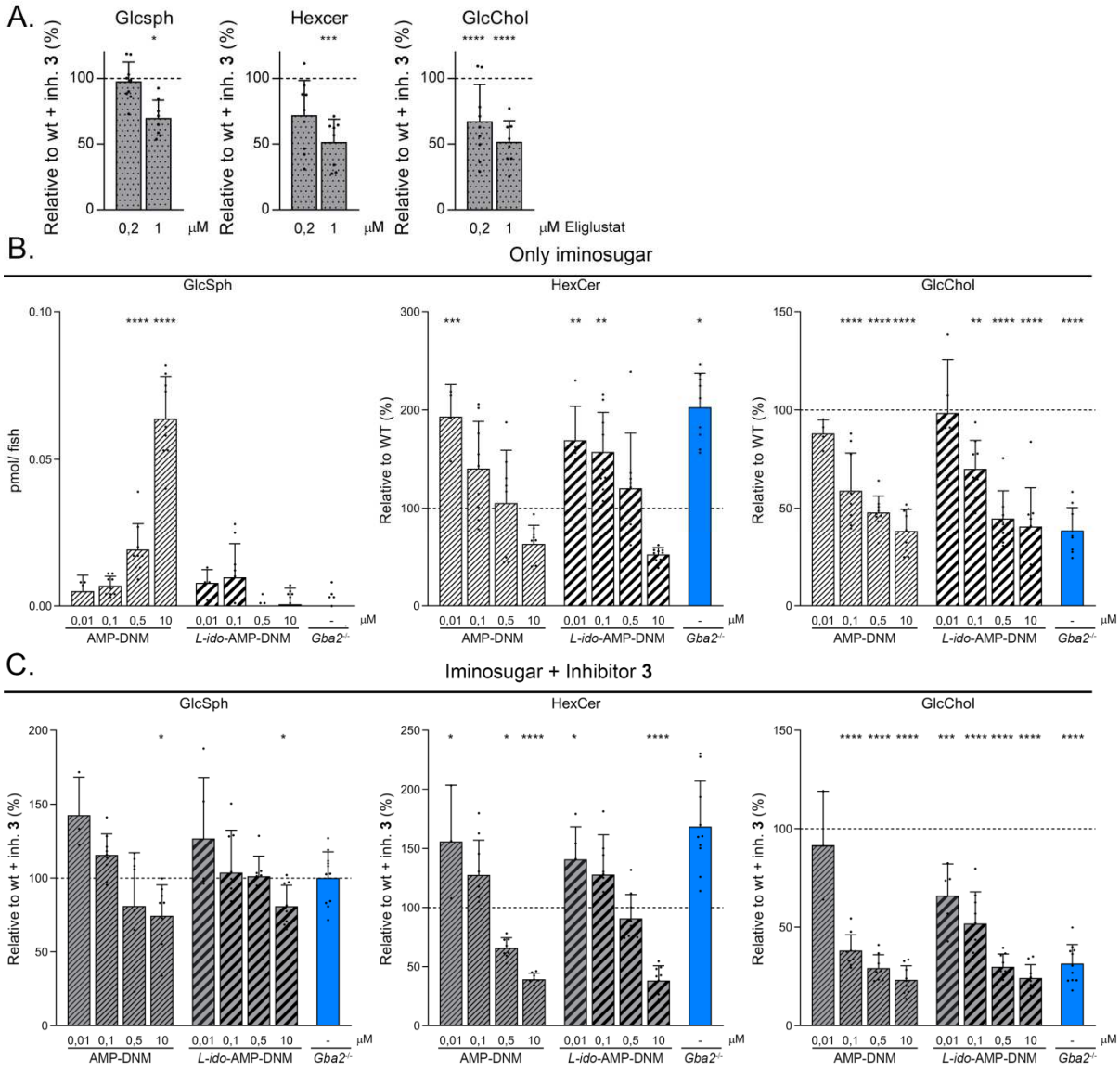

Figure 6 | Pharmacological inhibition of Gba1, Gba2 and Gcs

(A) WT embryos were treated simultaneously with inhibitor **3** and Eliglustat. Lipid levels were determined of individual larvae (n = 8-9). Ratios of GlcSph, HexCer and GlcChol are depicted relative to WT embryos incubated with inhibitor 1 only (100% line). (B) WT embryos were incubated for 5 days with different concentrations of AMP-DNM (striped bars) or L-*ido*-AMP-DNM (thicker striped bars) and lipid levels were determined of individual larvae (n = 5-9). Data of GlcSph is depicted in pmol/larvae while ratios of HexCer and GlcChol are depicted relative to vehicle treated WT (100% line). (C) WT embryos were treated with inhibitor **3** (10 µM) and different concentrations of AMP-DNM (striped bars) or L-*ido*-AMP-DNM (thicker striped bars) and lipid levels were determined of individual larvae (n = 5-9). Data of GlcSph, HexCer and GlcChol is depicted relative to inhibitor **3**

treated WT (100% line). Inhibitor **3** treated *gba2*$^{-/-}$ (blue bar) is used as control for pharmacological Gba1 inhibition in a full genetic Gba2 deficient background. Data is depicted as mean ± SD and analysed by One-Way Anova (Dunnett's test) with WT as control group. * $P < 0.05$, ** $P < 0.01$, *** $P < 0.001$ and **** $P < 0.0001$.

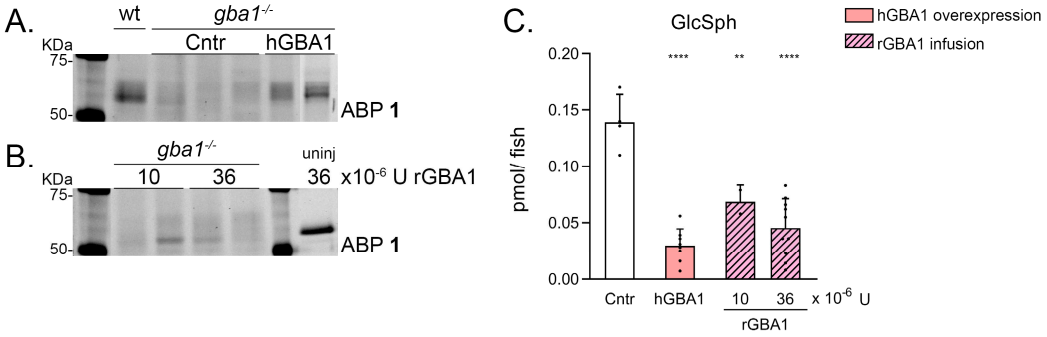

Figure 7 | Glycosphingolipid correction by introduction of human GBA1

(A) Human GBA1 was stably overexpressed in the g*ba1*$^{-/-}$ zebrafish background using the ubiquitin promoter. Zebrafish Gba1 and human GBA1 was visualized with ABP **1**. (B) Recombinant GBA1 was introduced by injection in the bloodstream of 2 dpf zebrafish with 10 or 36 x 10^{-6} U rGBA1 (Cerezyme®) and visualized with ABP **1**. An equivalent of 36 x 10^{-6} U rGBA1 was labelled and used as control on gel. (C) GlcSph levels were determined in pmol/ fish of uninjected, control *gba1*$^{-/-}$ zebrafish, *gba1*$^{-/-}$ zebrafish stably overexpressing hGBA1 and *gba1*$^{-/-}$ zebrafish infused with rGBA1. Data is depicted as mean ± SD and analysed by One-Way Anova (Dunnett's test) with WT as control group. ** $P < 0.01$ and **** $P < 0.0001$.